Electronic Supplementary Material (ESI) for Physical Chemistry Chemical Physics.

The decisive role of 4f-covalency in structural direction and oxidation state of XPrO compounds (X: groups 13 to 17 elements)

Wen-Jing Zhang,[1] Guan-Jun Wang,[2] Ping Zhang,[3] Wenli Zou,[4] Shu-Xian Hu,*[1,5]

[1] Beijing Computational Science Research Center, Beijing 100193, China, [2] Department of Chemistry, Shanghai Key Laboratory of Molecular Catalysts and Innovative Materials, Fudan University, Shanghai 200433, China, [3] Laboratory of Computational Physics, Institute of Applied Physics and Computational Mathematics, Beijing 100088, China, [4] Institute of Modern Physics, Northwest University, and Shaanxi Key Laboratory for Theoretical Physics Frontiers, Xi'an, 710127, China, [5] Department of Physics, University of Science and Technology Beijing, Beijing 100083, China.

*Corresponding Authors: hushuxian@csrc.ac.cn (S.X.H)

Table S1. Spin multiplicity, electronic configuration, state calculated relative energies (kcal mol^{-1}) and geometries (bond lengths in Å, bond angles in degrees) of the BPrO and BOPr molecule and oxidation state of Pr at the B3LYP levels of theory.

Structure	BOPr	BOPr	BPrO	BOPr
2S+1	5	3	5	7
State	^{5}A''	$^3\Delta$	^{5}A''	$^7\Sigma$
ΔE (B3LYP)	0.00	3.18	44.20	77.60
ΔE(CCSD(T))	0.00	3.55		
ΔE(DLPNO-CCSD(T))	0.00	23.88	62.87	109.78
Electronic configuration	$f^2 5d^1 6s^1 \sigma_{2s}^2$	$f_\delta^1 f_{\delta'}^1 \sigma^2$	$f_\delta^1 f_{\delta'}^1 \sigma^1 \pi_{//}^1 \pi_\perp^0$	$s^1 d_\pi^1 d_{\pi'}^1 f_\pi^1 f_{\pi'}^1 \sigma^1 \pi_{//}^0 \pi_\perp^0$
OS	Ⅰ	Ⅲ	Ⅲ	0
Symm.	C_s	$C_{\infty v}$	C_s	$C_{\infty v}$
E(B3LYP)	-563.18	-560.00	-518.98	-485.58
SOC	-14.61	-16.13	-13.97	-15.74
ΔE (B3LYP+SOC)	0.00	1.66	44.84	76.47
rPr-O	2.194	2.136	1.831	2.265
rB-Pr			2.497	
rB-O	1.278	1.290		1.259
∠B-Pr-O			113.9	
∠B-O-Pr	164.2	180.0		180.0
νPr-O	403.5	417.7	811.5	270.0
νB-Pr			313.9	
ν(cm^{-1})B-O	1510.5	1455.3		1469.9

Table S2. Spin multiplicity, electronic configuration, state calculated relative energies (kcal mol^{-1}) and geometries (bond lengths in Å, bond angles in degrees) of the AlPrO and AlOPr molecule and oxidation state of Pr at the B3LYP levels of theory.

Structure	AlOPr			AlPrO	AlOPr
2S+1	3	5	3	5	7
State	$^3\Sigma$	$^5\Phi$	$^3\Sigma$	^{5}A'	$^7\Gamma$
ΔE(B3LYP)	0.00	16.04	30.33	30.78	76.84
ΔE(DLPNO-CCSD(T))	0.00	22.48	0.10	34.38	93.36
Electronic configuration	$s^2 f_\delta^1 f_{\delta'}^1 \sigma^2 \pi_{//}^0 \pi_\perp^0$	$s^1 d_\pi^1 f_\pi^1 f_\phi^1 \sigma^2 \pi_{//}^0 \pi_\perp^0$	$s^2 f_\phi^1 f_{\phi'}^1 \sigma^2 \pi_{//}^0 \pi_\perp^0$	$f_\phi^1 f_{\phi'}^1 \sigma^1 \pi_{//}^1 \pi_\perp^0$	$s^1 d_\delta^1 f_\delta^1 f_\phi^1 \sigma^1 \pi_{//}^1 \pi_\perp^0$
OS	Ⅰ	Ⅰ	Ⅰ	Ⅲ	Ⅰ
Symm.	$C_{\infty v}$	$C_{\infty v}$	$C_{\infty v}$	C_s	$C_{\infty v}$
E(B3LYP)	-522.66	-506.62	-492.33	-491.88	-445.82
SOC	-8.23	-8.26	-8.23	-14.20	-8.27
ΔE (B3LYP+SOC)	0.00	16.01	30.33	24.81	76.80
rPr-O	2.104	2.163	2.107	1.839	2.173
rAl-Pr				3.099	
rAl-O	1.747	1.739	1.750		1.719
∠Al-Pr-O				96.1	
∠Al-O-Pr	180.0	180.0	180.0		180.0

ν(cm^{-1})Pr-O				803.5	
ν(cm^{-1})Al-Pr				178.6	
ν3(cm^{-1})	853.6	848.5	848.8		883.5
ν1(cm^{-1})	338.6	315.8	337.3		313.8

Table S3. Spin multiplicity, electronic configuration, state calculated relative energies (kcal mol^{-1}) and geometries (bond lengths in Å, bond angles in degrees) of the CPrO molecule and oxidation state of Pr at the B3LYP levels of theory.

2S+1	4	4	6
State	$^4\Gamma$	$^4\Phi$	^{6}A'
ΔE(B3LYP)	0.00	5.21	6.03
ΔE(CCSD(T))	14.00		0.00
ΔE(DMRG-CASPT2)	16.60		0.00
ΔE(DLPNO-CCSD(T))	7.16	7.28	0.00
Electronic configuration	$f_\phi^1\sigma^1\pi_{//}^2\pi_\perp^1$	$f_\delta^1\sigma^1\pi_{//}^2\pi_\perp^1$	$f_\delta^1f_{\delta'}^1\sigma^1\pi_{//}^1\pi_\perp^1$
OS	Ⅳ	Ⅳ	Ⅲ
Symm.	$C_{\infty v}$	$C_{\infty v}$	C_s
E(B3LYP)	-558.57	-553.36	-552.54
SOC	-15.89	-15.98	-16.98
ΔE (B3LYP+SOC)	0.00	5.12	4.94
rPr-O	1.819	1.808	1.823
rC-Pr	2.008	1.994	2.441
∠C-Pr-O	180.0	180.0	123.8
ν(cm^{-1})Pr-O	781.6	799.3	820.9
ν(cm^{-1})C-Pr	589.8	603.3	415.6

Table S4. Spin multiplicity, electronic configuration, state calculated relative energies (kcal mol^{-1}) and geometries (bond lengths in Å, bond angles in degrees) of the SiPrO and SiOPr molecule and oxidation state of Pr at the B3LYP levels of theory.

Structure	SiOPr		SiPrO		SiOPr
2S+1	4	6	6	4	8
State	^{4}A''	^{6}A'	^{6}A'	^{4}A''	$^8\Delta$
ΔE(B3LYP)	0.00	5.65	16.15	26.40	95.92
ΔE(DLPNO-CCSD(T))	0.00	8.17	12.68	34.58	108.69
Electronic configuration	$f_\phi^1f_\pi^1\pi_{Si}^1$	$s^1f_\delta^1f_{\delta'}^1d^1\sigma^1$	$f_\phi^1f_{\phi'}^1\sigma^1\pi_{//}^1\pi_\perp^1$	$f_\phi^1\sigma^1\pi_{//}^2\pi_\perp^1$	$s^1f_\pi^1f_{\pi'}^1d^1\sigma^1\pi_{//}^1\pi_\perp^1$
OS	Ⅱ	Ⅰ	Ⅲ	Ⅳ	Ⅰ
Symm.	C_s	C_s	C_s	C_s	$C_{\infty v}$
E(B3LYP)	-548.13	-542.48	-531.98	-521.73	-452.21
SOC	-14.41	-14.36	-13.89	-13.73	-16.27
ΔE (B3LYP+SOC)	0.00	5.70	16.67	27.08	94.06
rPr-O	2.030	2.090	1.840	1.829	2.127
rSi-Pr	2.842	2.876	2.972	2.610	

rSi-O	1.736	1.703			1.668
∠Si-Pr-O			169.0	120.9	
∠Si-O-Pr	97.7	98.1			180.0
ν(cm^{-1})Pr-O			810.5	797.9	
ν(cm^{-1})Si-Pr			218.6	313.8	
ν3(cm^{-1})	484.0	418.7			881.5
ν1(cm^{-1})	667.7	721.5			315.4

Table S5. Spin multiplicity, electronic configuration, oxidation state of Pr, symmetry, Calculated relative energies (kcal mol^{-1}) and geometries (bond lengths in Å, bond angles in degrees) of the neutral NPrO molecule at the B3LYP levels of theory. And the comparison between the observed and calculated vibrational frequencies (cm^{-1}) of NPrO.

2S+1	1	3	5	Expl.[ref1]	B3LYP[ref1]
State	$^1\Sigma$	$^3\Delta$	^{5}A''		
ΔE(B3LYP)	0.00	12.89	48.78		
ΔE(DLPNO-CCSD(T))	0.00	20.50	52.35		
Electronic configuration	$f^0\sigma^2\pi_{//}^2\pi_\perp^2$	$f_\delta^1\sigma^1\pi_{//}^2\pi_\perp^2$	$f_\delta^1f_{\delta'}^1\sigma^1\pi_{//}^2\pi_\perp^1$		$f^0\sigma^2\pi_{//}^2\pi_\perp^2$
OS	Ⅴ	Ⅳ	Ⅲ	Ⅴ	Ⅴ
Symm.	$C_{\infty v}$	$C_{\infty v}$	C_s		
E(B3LYP)	-671.36	-658.47	-622.58		
SOC	-12.53	-12.44	-13.68		
ΔE (B3LYP+SOC)	0.00	12.98	47.63		
rPr-O	1.798	1.829	1.853		1.765
rN-Pr	1.708	1.808	2.219		1.677
∠N-Pr-O	180.0	180.0	116.4		180.0
ν(cm^{-1})Pr-O	818.7	731.6	795.4	762.2/755.9[a]	822.1
ν(cm^{-1})N-Pr	1016.8	821.0	446.1	926.2/918.5[a]	1021.1

[a]Two site absorptions.

Table S6. Spin multiplicity, electronic configuration, state calculated relative energies (kcal mol^{-1}) and geometries (bond lengths in Å, bond angles in degrees) of the PPrO molecule and oxidation state of Pr at the B3LYP levels of theory.

2S+1	3	5	1
State	$^3\Delta$	^{5}A''	^{1}A'
ΔE (B3LYP)	0.00	7.37	15.84
ΔE (CCSD(T))	0.00	12.76	
ΔE(DLPNO-CCSD(T))	0.00	2.46	16.78
Electronic configuration	$f_\delta^1\sigma^1\pi_{//}^2\pi_\perp^2$	$f_\delta^1f_{\delta'}^1\sigma^1\pi_{//}^2\pi_\perp^1$	$f^0\sigma^2\pi_{//}^2\pi_\perp^2$
OS	Ⅳ	Ⅲ	Ⅴ
Symm.	$C_{\infty v}$	C_s	C_s
E(B3LYP)	-563.66	-556.29	-547.82
SOC	-16.05	-14.76	-13.65

ΔE (B3LYP+SOC)	0.00	8.66	18.24
rPr-O	1.815	1.841	1.796
rP-Pr	2.383	2.756	2.297
∠P-Pr-O	180.0	119.9	161.0
ν(cm^{-1})Pr-O	816.7	812.5	851.8
ν(cm^{-1})P-Pr	386.3	290.2	448.5

Table S7. Spin multiplicity, electronic configuration, state calculated relative energies (kcal mol^{-1}) and geometries (bond lengths in Å, bond angles in degrees) of the AsPrO molecule and oxidation state of Pr at the B3LYP levels of theory.

2S+1	3	5	5
State	$^3\Phi$	^{5}A'	^{5}A'
ΔE(B3LYP)	0.00	0.17	27.04
ΔE(CCSD(T))	35.82	0.00	
ΔE(DLPNO-CCSD(T))	23.56	0.00	8.31
Electronic configuration	$f_\phi^1\sigma^1\pi_{//}^2\pi_\perp^2$	$f_\delta^1f_\phi^1\sigma^1\pi_{//}^1\pi_\perp^2$	$d_\pi^1f_\sigma^1\sigma^1\pi_{//}^1\pi_\perp^2$
OS	Ⅳ	Ⅲ	Ⅲ
Symm.	$C_{\infty v}$	C_s	C_s
E(B3LYP)	-554.44	-552.74	-527.40
SOC	-17.40	-15.96	-15.79
ΔE (B3LYP+SOC)	0.00	3.14	28.65
rPr-O	1.822	1.841	2.050
rAs-Pr	2.511	3.023	2.909
∠As-Pr-O	180.0	109.8	39.95
ν(cm^{-1})Pr-O	804.9	811.0	499.7 (ν_3)
ν(cm^{-1})As-Pr	261.5	161.1	580.2 (ν_1)

Table S8. Spin multiplicity, electronic configuration, oxidation state of Pr, symmetry, Calculated relative energies (kcal mol^{-1}) and geometries (bond lengths in Å, bond angles in degrees) of the neutral PrO_2 molecule at the B3LYP levels of theory. And the comparison between the observed and calculated vibrational frequencies (cm^{-1}) of PrO_2.

2S+1	2	4	Expl.[ref2]	B3LYP[ref2]
State	$^2\Delta_u$	$^4A_2$		
ΔE(B3LYP)	0.00	43.22		
ΔE(DLPNO-CCSD(T))	0.00	54.76		
Electronic configuration	$f_\delta^1\sigma^2\pi_{//}^2\pi_\perp^2$	$f_\delta^1f_\phi^1\sigma^1\pi_{//}^2\pi_\perp^2$		$f^1\sigma^2\pi_{//}^2\pi_\perp^2$
OS	Ⅳ	Ⅲ	Ⅳ	Ⅳ
Symm.	D_{2h}	C_{2v}		
E(B3LYP)	-659.75	-616.53		
SOC	-16.48	-16.27		
ΔE (B3LYP+SOC)	0.00	43.43		

rPr-O	1.812	1.938		1.810
rO-Pr	1.812	1.938		1.810
∠O-Pr-O	180.0	140.2		180.0
v3(cm^{-1})	812.1	229.0	694.2	783.2
v1(cm^{-1})	759.6	635.5	730.3	730.8

Table S9. Spin multiplicity, electronic configuration, oxidation state of Pr, symmetry, Calculated relative energies (kcal mol^{-1}) and geometries (bond lengths in Å, bond angles in degrees) of the neutral $[PrO_2]^+$ molecule at the B3LYP levels of theory. And the comparison between the observed and calculated vibrational frequencies (cm^{-1}) of $[PrO_2]^+$.

2S+1	1	3	5	Expl.[ref2]	B3LYP[ref2]
State	$^1\Sigma_u$	$^3\Delta_u$	$^5A_2$		
ΔE(B3LYP)	0.00	22.37	96.90		
ΔE(DLPNO-CCSD(T))	0.00	36.14	93.35		
Electronic configuration	$f^0\sigma^2\pi_{//}^2\pi_\perp^2$	$f_\delta^1\sigma^1\pi_{//}^2\pi_\perp^2$	$f_\delta^1f_{\delta'}^1\sigma^1\pi_{//}^2\pi_\perp^2\sigma^1\pi_{//}^2\pi_\perp^2$		$f^0\sigma^2\pi_{//}^2\pi_\perp^2$
OS	Ⅴ	Ⅳ	Ⅲ	Ⅴ	Ⅴ
Symm.	D_{2h}	D_{2h}	C_{2v}		$D_{\infty v}$
E(B3LYP)	-523.14	-500.77	-426.24		
SOC	-12.50	-12.29	-12.31		
ΔE (B3LYP+SOC)	0.00	22.58	97.09		
rPr-O	1.671	1.781	1.980		1.688
rO-Pr	1.671	1.781	1.980		1.688
∠O-Pr-O	180.0	180.0	125.1		180.0
v3(cm^{-1})	1128.6	739.7	453.0		1020.9
v1(cm^{-1})	991.4	755.0	643.4		882.0

Table S10. Spin multiplicity, electronic configuration, state calculated relative energies (kcal mol^{-1}) and geometries (bond lengths in Å, bond angles in degrees) of the SPrO molecule and oxidation state of Pr at the B3LYP levels of theory.

2S+1	2	4
State	$^2A'$	$^4\Sigma$
ΔE(B3LYP)	0.00	40.28
ΔE(DLPNO-CCSD(T))	0.00	19.94
Electronic configuration	$f_\phi^1\sigma^2\pi_{//}^2\pi_\perp^2$	$f_\delta^1f_{\delta'}^1\sigma^1\pi_{//}^2\pi_\perp^2$
OS	Ⅳ	Ⅲ
Symm.	C_s	$C_{\infty v}$
E(B3LYP)	-603.34	-563.06
SOC	-16.31	-16.04
ΔE (B3LYP+SOC)	0.00	40.55
rPr-O	1.817	1.856
rS-Pr	2.412	2.573

∠S-Pr-O	134.1	180.0
ν(cm^{-1})Pr-O	799.3	712.4
ν(cm^{-1})S-Pr	603.3	245.8

Table S11. Spin multiplicity, electronic configuration, state calculated relative energies (kcal mol^{-1}) and geometries (bond lengths in Å, bond angles in degrees) of the $[SPrO]^+$ molecule and oxidation state of Pr at the B3LYP levels of theory.

2S+1	3	3	1
State	$^3\Phi$	$^3\Delta$	$^1\Sigma$
ΔE(B3LYP)	0.00	1.61	1.74
ΔE(CCSD(T))	0.00	6.38	
ΔE(DLPNO-CCSD(T))	9.20	8.54	0.00
Electronic configuration	$f_\phi{}^1\sigma^1\pi_{//}{}^2\pi_\perp{}^2$	$f_\delta{}^1\sigma^1\pi_{//}{}^2\pi_\perp{}^2$	$f^0\sigma^2\pi_{//}{}^2\pi_\perp{}^2$
OS	Ⅳ	Ⅳ	Ⅴ
Symm.	$C_{\infty v}$	$C_{\infty v}$	$C_{\infty v}$
E(B3LYP)	-415.16	-413.55	-413.42
SOC	-12.33	-12.31	-12.27
ΔE (B3LYP+SOC)	0.00	1.63	1.80
rPr-O	1.765	1.757	1.731
rS-Pr	2.383	2.368	2.259
∠S-Pr-O	180.0	180.0	180.0
ν(cm^{-1})Pr-O	876.4	893.3	941.4
ν(cm^{-1})S-Pr	356.5	364.4	478.9

Table S12. Spin multiplicity, electronic configuration, oxidation state of Pr, symmetry, Calculated relative energies (kcal mol^{-1}) and geometries (bond lengths in Å, bond angles in degrees) of the neutral FPrO molecule at the B3LYP levels of theory. And the comparison between the observed and calculated vibrational frequencies (cm^{-1}) of FPrO .

2S+1	3	3	3	5	Expl.[ref3]	B3LYP[ref3]
State	$^3A''$	$^3A''$	$^3A'$	$^5A''$		
ΔE(B3LYP)	0.00	0.22	0.83	66.49		
ΔE(DLPNO-CCSD(T))	0.00	0.39	3.00	64.65		
Electronic configuration	$f_\delta{}^1f_{\delta'}{}^1\sigma^2\pi_{//}{}^2\pi_\perp{}^2$	$f_\phi{}^1f_{\phi'}{}^1\sigma^2\pi_{//}{}^2\pi_\perp{}^2$	$f_\delta{}^1f_\phi{}^1\sigma^2\pi_{//}{}^2\pi_\perp{}^2$	$s^1f_\delta{}^1f_{\delta'}{}^1\sigma^2\pi_{//}{}^2\pi_\perp{}^1$		$f^2\sigma^2\pi_{//}{}^2\pi_\perp{}^2$
OS	Ⅲ	Ⅲ	Ⅲ	Ⅱ	Ⅲ	Ⅲ
Symm.	C_s	C_s	C_s	C_s		
E(B3LYP)	-648.25	-648.03	-647.42	-581.76		
E(B3LYP)	-648.25	-648.03	-647.42	-581.76		
SOC	-13.95	-13.95	-13.95	-16.13		
ΔE (B3LYP+SOC)	0.00	0.22	0.83	64.31		
rPr-O	1.855	1.855	1.855	2.163		1.836
rF-Pr	2.133	2.134	2.134	2.059		2.122

∠F-Pr-O	114.2	114.6	114.7	114.4		114.1
ν(cm^{-1})Pr-O	798.1	794.2	777.3	501.5	767.5	794.0
ν(cm^{-1})F-Pr	474.9	478.2	461.7	545.8	451.2	502.0

Table S13. Spin multiplicity, electronic configuration, state calculated relative energies (kcal mol^{-1}) and geometries (bond lengths in Å, bond angles in degrees) of the F_3PrO molecule and oxidation state of Pr at the B3LYP levels of theory.

2S+1	1	3	5
State	^{1}A'	^{3}A''	^{5}A'
ΔE(B3LYP)	0.00	14.53	61.61
ΔE(DLPNO-CCSD(T))	0.00	10.56	83.80
Electronic configuration	$f^0\sigma^2\pi_{//}^2\pi_{\perp}^2$	$f_{\pi}^1\sigma^2\pi_{//}^2\pi_{\perp}^1$	$f_{\delta}^1f_{\delta'}^1\sigma^2\pi_{//}^1\pi_{\perp}^1$
OS	Ⅴ	Ⅳ	Ⅲ
Symm.	C_s	C_s	C_s
E(B3LYP)	-957.88	-943.35	-896.27
SOC	-12.45	-14.15	-15.83
ΔE (B3LYP+SOC)	0.00	12.83	58.23
rPr-O	1.794	2.142	2.869
rF-Pr	2.048	2.051	2.113
∠F-Pr-O	113.0, 116.7	107.2,113.7	88.7,116.3
ν(cm^{-1})Pr-O	813.4	446.4	153.8
ν(cm^{-1})F-Pr	564.2	551.7	503.7

Table S14. Spin multiplicity, electronic configuration, state calculated relative energies (kcal mol^{-1}) and geometries (bond lengths in Å, bond angles in degrees) of the ClPrO molecule and oxidation state of Pr at the B3LYP levels of theory.

2S+1	3	3	3	5
State	^{3}A''	^{3}A''	^{3}A'	^{5}A''
ΔE(B3LYP)	0.00	0.17	1.12	72.84
ΔE(DLPNO-CCSD(T))	0.00	2.66	0.03	72.99
Electronic configuration	$f_{\delta}^1f_{\delta'}^1\sigma^2\pi_{//}^2\pi_{\perp}^2$	$f_{\phi}^1f_{\phi'}^1\sigma^2\pi_{//}^2\pi_{\perp}^2$	$f_{\delta}^1f_{\phi}^1\sigma^2\pi_{//}^2\pi_{\perp}^2$	$s^1f_{\phi}^1f_{\phi'}^1\sigma^1\pi_{//}^2\pi_{\perp}^2$
OS	Ⅲ	Ⅲ	Ⅲ	Ⅱ
Symm.	C_s	C_s	C_s	C_s
E(B3LYP)	-590.19	-590.02	-589.07	-517.35
SOC	-16.97	-16.98	-16.14	-14.06
ΔE (B3LYP+SOC)	0.00	0.16	1.95	75.75
rPr-O	1.841	1.842	1.842	2.025
rCl-Pr	2.654	2.652	2.654	2.582
∠Cl-Pr-O	118.9	117.3	117.8	157.9
ν(cm^{-1})Pr-O	811.4	816.1	806.3	502.1
ν(cm^{-1})Cl-Pr	293.4	296.3	282.6	299.4

Table S15. Spin multiplicity, electronic configuration, state calculated relative energies (kcal mol^{-1}) and geometries (bond lengths in Å, bond angles in degrees) of the Cl_3PrO molecule and oxidation state of Pr at the B3LYP levels of theory.

2S+1	1	3
State	$^1A'$	$^3A''$
ΔE(B3LYP)	0.00	18.90
ΔE(DLPNO-CCSD(T))	0.00	15.79
Electronic configuration	$f^0\sigma^2\pi_{//}{}^2\pi_{\perp}{}^2$	$f_\pi{}^1\sigma^2\pi_{//}{}^2\pi_{\perp}{}^1$
OS	Ⅴ	Ⅳ
Symm.	C_s	C_s
E(B3LYP)	-771.59	-752.69
SOC	-12.68	-13.32
ΔE (B3LYP+SOC)	0.00	18.26
rPr-O	1.773	2.094
rCl-Pr	2.518	2.515
∠Cl-Pr-O	111.7,117.6	106.8,113.1
ν(cm^{-1})Pr-O	848.8	525.4
ν(cm^{-1})Cl-Pr	331.8	340.7

Table S16. The Natural Localized Molecular Orbital Analysis of the Bonds in XPrO (X: C, Si, N, P, As, O, S, F and Cl) Complexes

Species	Pr-O/X	NLMO	| ΘA-ΘB |
CPrO	Pr-O	76.50% $O(sp^{8.00})$ +23.48%$Pr(s^{0.02}d^{1.37}f)$	53.02
		85.68% $O(sp^{1.00})$ +14.29%$Pr(s^{0.05}d^{3.42}f)$	71.39
		85.89% $O(sp^{99.99})$ +14.04%$Pr(s^{0.03}d^{2.42}f)$	71.85
	Pr-C	88.64% $C(sp^{1.00})$ +11.30%$Pr(s^{0.43}d^{11.44}f)$	77.34
		84.48% $C(sp^{6.64})$ +15.47%$Pr(s^{0.85}d^{2.86}f)$	69.01
NPrO	Pr-O	85.29% $O(sp^{1.00})$ +14.70%$Pr(s^{0.02}d^{0.94}f)$	70.59
		85.29% $O(sp^{1.00})$ +14.70%$Pr(s^{0.02}d^{0.94}f)$	70.59
		65.39% $O(sp^{7.17})$ +32.67%$Pr(s^{0.03}d^{0.42}f)$	32.72
	Pr-N	70.96% $N(sp^{1.00})$ +29.04%$Pr(s^{0.01}d^{0.89}f)$	41.92
		70.96% $N(sp^{1.00})$ +29.04%$Pr(s^{0.01}d^{0.89}f)$	41.92
		35.19% $N(sp^{8.58})$ +62.28%$Pr(s^{0.03}d^{0.26}f)$	27.09
OPrO	Pr-O	87.52% $O(sp^{1.00})$ +12.46%$Pr(s^{0.04}d^{1.40}f)$	75.06
		87.52% $O(sp^{1.00})$ +12.46%$Pr(s^{0.04}d^{1.40}f)$	75.06
		69.94% $O(sp^{7.88})$ +29.38%$Pr(s^{0.03}d^{0.35}f)$	40.56
	Pr-O	87.52% $O(sp^{1.00})$ +12.46%$Pr(s^{0.04}d^{1.40}f)$	75.06
		87.52% $O(sp^{1.00})$ +12.46%$Pr(s^{0.04}d^{1.40}f)$	75.06
		69.94% $O(sp^{7.88})$ +29.38%$Pr(s^{0.03}d^{0.35}f)$	40.56
$[OPrO]^+$	Pr-O	81.46% $O(sp^{1.00})$ +18.51%$Pr(s^{0.01}d^{1.00}f)$	62.95

		81.46% O($sp^{1.00}$) +18.51%Pr($s^{0.01}d^{1.00}f$)	62.95
		56.64% O($sp^{6.46}$) +41.37%Pr($s^{0.02}d^{0.31}f$)	15.27
	Pr-O	81.46% O($sp^{1.00}$) +18.51%Pr($s^{0.01}d^{1.00}f$)	62.95
		81.46% O($sp^{1.00}$) +18.51%Pr($s^{0.01}d^{1.00}f$)	62.95
		56.64% O($sp^{6.46}$) +41.37%Pr($s^{0.02}d^{0.31}f$)	15.27
FPrO	Pr-O	80.27% O($sp^{6.56}$) +19.72%Pr($s^{0.01}d^{1.37}f$)	60.55
		87.36% O($sp^{1.00}$) +12.64%Pr($s^{0.09}d^{4.62}f$)	74.72
		86.64% O($sp^{99.99}$) +13.34%Pr($s^{0.03}d^{2.59}f$)	73.30
	Pr-F	94.23% F($sp^{4.40}$) +5.73%Pr($s^{0.41}d^{3.69}f$)	88.50
F_3PrO	Pr-O	62.75% O($sp^{11.33}$) +37.23%Pr($s^{0.01}d^{1.00}f$)	25.52
		80.64% O($sp^{1.00}$) +19.30%Pr($s^{0.01}d^{0.69}f$)	61.34
		80.23% O($sp^{99.99}$) +19.72%Pr($s^{0.01}d^{0.63}f$)	60.51
	Pr-F(F_3)	89.14% F($sp^{4.54}$) +10.80%Pr($s^{0.11}d^{0.95}f$)	78.34
		89.14% F($sp^{4.54}$) +10.80%Pr($s^{0.11}d^{0.95}f$)	78.34
		89.04% F($sp^{4.61}$) +10.95%Pr($s^{0.09}d^{0.90}f$)	78.09
		93.17% F($sp^{99.99}$) +6.68%Pr($s^{0.01}d^{0.01}f$)	86.49
PPrO	Pr-O	87.59% O($sp^{1.00}$) +12.27%Pr($s^{0.02}d^{1.87}f$)	75.32
		75.27% O($sp^{6.90}$) +18.68%Pr($s^{0.12}d^{2.95}f$)	56.59
		98.26% O($sp^{0.09}$) +1.50%Pr($s^{20.00}d^{16.40}f$)	96.76
	Pr-P	80.51% P($sp^{1.00}$) +19.42%Pr($s^{0.07}d^{2.27}f$)	61.09
		34.21% P($sp^{27.66}$) +62.30%Pr($s^{0.01}d^{0.01}f$)	28.09
		98.12% P($sp^{0.03}$) +1.75%Pr($s^{9.09}d^{7.45}f$)	96.37
SPrO	Pr-O	81.46% O($sp^{7.89}$) +18.48%Pr($s^{0.03}d^{1.32}f$)	62.98
		86.76% O($sp^{1.00}$) +13.18%Pr($s^{0.03}d^{2.45}f$)	73.58
		84.84% O($sp^{27.17}$) +15.09%Pr($s^{0.01}d^{1.00}f$)	69.75
	Pr-S	89.58% S($sp^{99.99}$) +10.36%Pr($s^{0.01}d^{30.01}f$)	79.22
		87.97% S($sp^{1.00}$) +11.97%Pr($s^{0.07}d^{3.79}f$)	76.00
		83.90% S($sp^{4.80}$) +16.04%Pr($s^{0.36}d^{2.40}f$)	67.86
$[SPrO]^+$	Pr-O	82.70% O($sp^{1.00}$) +17.26%Pr($s^{0.01}d^{1.00}f$)	65.44
		82.70% O($sp^{1.00}$) +17.26%Pr($s^{0.01}d^{1.00}f$)	65.44
		59.48% O($sp^{8.75}$) +37.61%Pr($s^{0.01}d^{0.34}f$)	21.87
	Pr-S	78.03% S($sp^{1.00}$) +21.97%Pr($s^{0.03}d^{0.97}f$)	56.06
		78.03% S($sp^{1.00}$) +21.97%Pr($s^{0.03}d^{0.97}f$)	56.06
		47.14% S($sp^{22.16}$) +49.95%Pr($s^{0.01}d^{1.00}f$)	2.81
ClPrO	Pr-O	87.37% O($sp^{1.00}$) +12.63%Pr($s^{0.07}d^{3.94}f$)	74.74
		79.56% O($sp^{1.00}$) +20.42%Pr($s^{0.02}d^{1.89}f$)	59.14
		87.80% O($sp^{99.99}$) +12.14%Pr($s^{0.02}d^{1.78}f$)	75.66
	Pr-Cl	92.48% Cl($sp^{5.70}$) +7.46%Pr($s^{1.41}d^{5.65}f$)	85.02
Cl_3PrO	Pr-O	66.27% O($sp^{9.00}$) +33.69%Pr($s^{0.01}d^{1.00}f$)	32.58

		79.50% O($sp^{99.99}$) +20.43%Pr($s^{0.01}d^{0.01}f$)	59.07
		79.92% O($sp^{1.00}$) +20.01%Pr($s^{0.01}d^{1.00}f$)	59.91
	Pr-Cl(Cl_3)	86.25% Cl($sp^{10.37}$) +13.55%Pr($s^{0.18}d^{1.08}f$)	72.70
		90.50% Cl($sp^{99.99}$) +9.29%Pr($s^{0.01}d^{1.00}f$)	81.21
		88.51% Cl($sp^{12.00}$) +11.31%Pr($s^{0.17}d^{1.40}f$)	77.20
		84.73% Cl($sp^{8.21}$) +15.15%Pr($s^{0.17}d^{1.05}f$)	69.58
		90.85% Cl($sp^{1.00}$) +8.86%Pr($s^{0.01}d^{0.01}f$)	81.99
		89.48% Cl($sp^{16.17}$) +10.30%Pr($s^{0.13}d^{1.28}f$)	79.18
AsPrO	Pr-O	85.32% O($sp^{1.00}$) +14.67%Pr($s^{0.04}d^{3.38}f$)	75.32
		84.20% O($sp^{45.43}$) +15.78%Pr($s^{0.01}d^{1.20}f$)	68.42
		78.80% O($sp^{9.82}$) +21.17%Pr($s^{0.01}d^{0.01}f$)	57.63
	Pr-As	96.05% As($sp^{99.99}$) +3.83%Pr($s^{0.09}d^{2.69}f$)	92.22
		94.94% As($sp^{1.00}$) +5.01%Pr($s^{3.23}d^{82.42}f$)	89.93
		81.86% As($sp^{18.50}$) +18.07%Pr($s^{11.11}d^{9.22}f$)	63.79

Table S17. The Natural Localized Molecular Orbital Analysis of the Bonds in XOPr (X: B, Al and Si) Complexes

Species	Pr-O/X	NLMO	| ΘA-ΘB |
BOPr	B-O	85.84% O($sp^{0.81}$) +14.01%B($sp^{14.89}$)	71.83
		89.87% O($sp^{1.00}$) +8.43%B($sp^{1.00}$)	81.44
		89.86% O($sp^{99.99}$) +8.34%B($sp^{99.99}$)	81.52
	Pr-O	96.79% O($sp^{1.23}$) +3.01%Pr($s^{0.41}d^{6.27}f$)	93.78
AlOPr	Al-O	93.69% O($sp^{1.00}$) +3.42%Al($sp^{1.00}$)	90.27
		96.22% O($sp^{0.01}$) +1.89%Al($sd^{11.63}$)	94.33
	Pr-O	93.21% O($sp^{99.99}$) +3.48%Pr($s^{0.22}d^{4.43}f$)	89.73
SiOPr	Si-O	86.45% O($sp^{3.56}$) +12.37%Si($sp^{9.93}$)	74.08
		88.08% O($sp^{1.00}$) +7.75%Si($sp^{1.00}$)	80.33
	Pr-O	90.69% O($sp^{8.32}$) +8.83%Pr($s^{0.06}d^{4.41}f$)	81.86
	Pr-Si	60.23% Si($sp^{21.98}$) +39.67%Pr($s^{50.00}d^{19.00}f$)	20.56

Table S18. Correlation of Pr oxidation state and the σ-component (%Pr) of NLMO in X−Pr as well as the corresponding contribution ratio of 4f:5d.

σ-bond	4f:5d	OS(Pr)	%Pr
C−Pr	0.3497	III	27.91
N−Pr	3.8462	V	62.28
O−Pr	2.8571	IV	29.38
O−Pr ($[OPrO]^+$)	3.2258	V	41.37
F−Pr	0.2710	III	5.73
F−Pr ($[F_3PrO]$)	1.0526	V	10.95

P−Pr	0.4405	IV	19.42
S−Pr	0.4167	IV	16.04
S−Pr ([SPrO]$^+$)	1.0000	V	49.95
Cl−Pr	0.1770	III	7.46
Cl−Pr ([Cl_3PrO])	1.1013	V	13.69
As−Pr	0.1085	III	18.07

Table S19. Energy decomposition analysis of ground state XPrO at the B3LYP/TZ2P level. Energy values are given in kcal/mol.

	EDA				ETS-NOCV					
Species	ΔE_{int}	ΔE_{Pauli}	ΔE_{elstat}	ΔE_{orb}	ΔE_1^{orb}	ΔE_2^{orb}	ΔE_3^{orb}	Contours		
								Orb1	Orb2	Orb3
CPrO	-300.09	151.58	-215.11	-236.56	-49.1	-55.0	-71.6	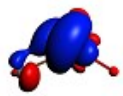		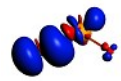
NPrO	-1513.50	922.33	-1562.53	-873.30	-178.7	-112.0	-112.0	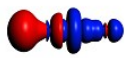		
OPrO	-771.33	603.66	-936.85	-438.14	-85.0	-93.9	-41.3	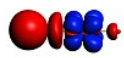		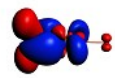
[OPrO]$^+$	-1123.09	871.16	-1321.40	-672.85	-154.9	-77.5	-77.5			
FPrO	-268.27	149.49	-258.25	-159.51	-41.9	-36.7	-18.1	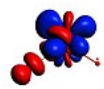	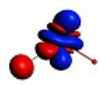	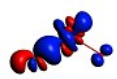
F_3PrO	-1434.10	369.05	-1375.85	-427.30	-41.3	-40.7	-27.2	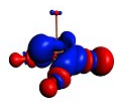		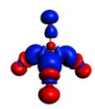
PPrO	-615.72	330.84	-602.54	-344.01	-86.4	-68.8	-68.8	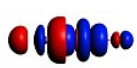	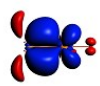	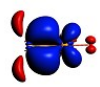
SPrO	-653.38	286.41	-640.13	-299.66	-93.5	-64.1	-36.3	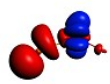	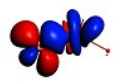	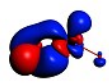
[SPrO]$^+$	-996.73	404.75	-903.61	-497.87	-108.2	-63.6	-63.6		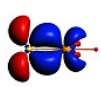	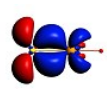
ClPrO	-222.02	92.57	-191.31	-123.28	-39.6	-37.9	-14.8	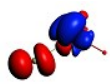	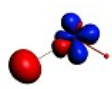	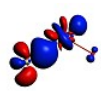

Cl_3PrO	-1259.39	264.70	-1061.79	-462.31	-45.8	-44.2	-29.6	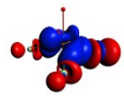	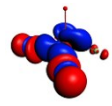	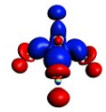
AsPrO	-252.80	78.38	-159.27	-171.91	-47.9	-49.9	-50.4	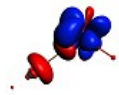	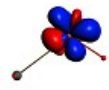	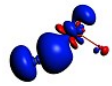

Table S20. Calculated charge and spin populations on X, Pr and O atoms of the XPrO molecule at the B3LYP levels of theory.

		Charge				Spin		
Species	Atom	Mulliken	Hirshfeld	NPA	MDC_q	Mulliken	NPA	MDC_q
BOPr	B	0.244	-0.094	0.416	0.150	-0.015	0.024	-0.169
	O	-0.666	-0.376	-1.257	-0.886	-0.074	-0.001	0.129
	Pr	0.422	0.470	0.841	0.736	4.089	3.977	4.039
CPrO	C	-0.567	-0.346	-0.610	-0.647	2.707	2.638	2.635
	O	-0.719	-0.557	-1.000	-1.073	-0.039	-0.041	-0.038
	Pr	1.286	0.903	1.611	1.720	2.332	2.403	2.403
NPrO	N	-0.578	-0.594	-0.726	-0.929	0.000	0.000	0.000
	O	-0.693	-0.515	-0.782	-0.718	0.000	0.000	0.000
	Pr	1.271	1.109	1.508	1.648	0.000	0.000	0.000
OPrO	O	-0.771	-0.547	-0.861	-0.820	-0.073	-0.061	-0.076
	Pr	1.542	1.095	1.722	1.641	1.145	1.123	1.152
$[OPrO]^+$	O(+)	-0.465	-0.312	-0.500	-0.457	0.000	0.000	0.000
	Pr	1.929	1.625	2.001	1.914	0.000	0.000	0.000
FPrO	F	-0.611	-0.42	-0.725	-0.809	-0.015	-0.012	0.019
	O	-0.690	-0.577	-1.037	-1.118	-0.073	-0.054	-0.03
	Pr	1.301	0.997	1.762	1.927	2.088	2.065	2.011
F_3PrO	$F(F_3)$	-0.490	-0.305	-0.513	-0.408	0.000	0.000	0.000
	O	-0.566	-0.341	-0.472	-0.328	0.000	0.000	0.000
	Pr	2.036	1.257	2.012	1.551	0.000	0.000	0.000
AlOPr	Al	0.521	0.266	0.768	0.061	0.004	-0.006	-0.001
	O	-0.711	-0.536	-1.515	-0.165	-0.021	-0.031	-0.029
	Pr	0.190	0.270	0.747	0.104	2.017	2.036	2.03
SiOPr	Si	0.209	0.047	0.411	0.410	0.016	-0.042	-0.030
	O	-0.637	-0.434	-1.218	-1.105	-0.074	-0.027	0.079
	Pr	0.429	0.388	0.807	0.695	3.058	3.069	2.951
PPrO	P	-0.672	-0.452	-0.595	-0.530	0.412	0.198	0.565
	O	-0.699	-0.518	-0.878	-0.497	-0.090	-0.134	0.009
	Pr	1.370	0.970	1.474	1.026	1.678	1.936	1.426
SPrO	S	-0.687	-0.505	-0.718	-0.748	-0.180	-0.512	-0.173
	O	-0.592	-0.501	-0.863	-1.005	-0.078	-0.191	-0.091

	Pr	1.278	1.006	1.581	1.753	1.258	1.703	1.263
$[SPrO]^+$	S(+)	-0.253	-0.123	-0.178	-0.152	0.000	0.000	0.000
	O	-0.495	-0.331	-0.605	-0.326	0.000	0.000	0.000
	Pr	1.748	1.454	1.783	1.478	0.000	0.000	0.000
ClPrO	Cl	-0.642	-0.398	-0.727	-0.633	-0.008	-0.008	-0.007
	O	-0.658	-0.558	-1.012	-1.103	-0.056	-0.084	-0.057
	Pr	1.300	0.957	1.739	1.736	2.064	2.093	2.064
Cl_3PrO	$Cl(Cl_3)$	-0.422	-0.193	-0.299	-0.496	0.000	0.000	0.000
	O	-0.510	-0.338	-0.489	-0.943	0.000	0.000	0.000
	Pr	1.775	0.919	1.386	2.426	0.000	0.000	0.000
AsPrO	As	-0.460	-0.252	-0.520	-0.383	1.903	1.940	1.934
	O	-0.621	-0.551	-1.010	-1.157	-0.050	-0.052	-0.058
	Pr	1.081	0.803	1.530	1.539	2.150	2.112	2.124

Table S21. Energies and percent compositions of the occupied valence molecular orbitals of BOPr at the B3LYP andM06-HF levels of theory.

					B3LYP				M06-HF			
MOs	Isosurface	type	Energy	Occ	Pr		O	B	Pr		O	B
					5d	4f	2p	2p	5d	4f	2p	2p
1a''	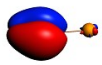	π_{Pr-O}	-10.339	2	3.19%		82.22%	11.72%	2.94%		69.49%	2.50%
2a'		π_{Pr-O}	-10.357	2	2.45%	1.08%	82.28%	11.57%	1.42%		84.81%	7.95%
1a'	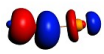	σ_{Pr-O}	-13.053	2	5.19%		72.12%	3.09%	1.93%		86.28%	8.08%

Table S22. Energies and percent compositions of the occupied valence molecular orbitals of AlOPr at the M06-HF levels of theory.

					B3LYP				M06-HF			
MOs	Isosurface	type	Energy	Occ	Pr		O	Al	Pr		O	Al
					5d	4f	2p	2p	5d	4f	2p	2p
3σ		Pr-6s	-3.933	2	7.89%				19.87%			
1δ'	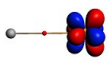	Pr-$4f_\delta$	-5.564	1		99.22%				97.46%		
1δ	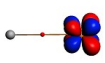	Pr-$4f_\delta$	-5.564	1		99.22%				97.46%		
2σ	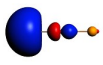	Al-3s	-6.223	2	2.29%		8.70%	14.85%	1.75%		4.71%	13.01%
1π'		π_{Pr-O}	-8.859	2	5.91%	1.32%	84.82%	4.70%	4.35%	3.00%	87.39%	2.38%

1π		π_{Pr-O}	-8.859	2	5.91%	1.32%	84.82%	4.70%	4.35%	3.00%	87.39%	2.38%
1σ	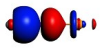	σ_{Pr-O}	-10.756	2	7.59%	1.77%	70.88%		10.01%	1.60%	67.91%	1.34%

Table S23. Energies and percent compositions of the occupied valence molecular orbitals of CPrO at the B3LYP and M06-HF levels of theory.

					B3LYP				M06-HF			
MOs	Isosurface	type	Energy	Occ	Pr		O	C	Pr		O	C
					5d	4f	2p	2p	5d	4f	2p	2p
3a''		Pr-4f	-5.138	1	4.36%	81.62%				96.47%		
5a'		Pr-4f	-5.145	1	3.24%	79.24%				94.18%	3.53%	
4a'		π_{C-Pr}	-5.589	1	2.35%	3.45%	5.01%	81.49%	2.61%		7.27%	84.77%
2a''		π_{C-Pr}	-5.910	1	6.85%	14.34%		75.24%	9.63%		1.63%	84.88%
3a'	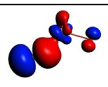	σ_{C-Pr}	-6.007	1	5.96%	11.62%		71.68%	5.93%		6.34%	77.04%
2a'	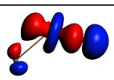	σ_{Pr-O}	-7.413	2	7.40%	6.17%	61.54%		18.65%	4.95%	63.36%	3.20%
1a''	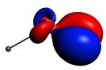	π_{Pr-O}	-7.809	2	11.03%	5.37%	77.02%		15.97%	1.48%	78.99%	
1a'		π_{Pr-O}	-7.853	2	10.44%	4.05%	72.87%		15.00%	1.84%	69.45%	7.54%

Table S24. Energies and percent compositions of the occupied valence molecular orbitals of SiOPr at the B3LYP and M06-HF levels of theory.

					B3LYP				M06-HF			
MOs	Isosurface	type	Energy	Occ	Pr		O	Si	Pr		O	Si
					5d	4f	2p	2p	5d	4f	2p	2p
5a'		π_{Si-Pr}	-3.742	1	45.15%	2.36%	4.43%	51.24%	38.81%		1.10%	8.32%
4a'	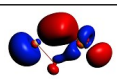	σ_{Si-Pr}	-4.257	2	17.82%		1.625	46.49%	13.83%		1.53%	56.97%
3a'		Pr-4f	-5.514	1		97.37%				86.14%	4.95%	
2a''	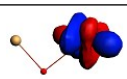	Pr-4f	-5.620	1		96.47%				98.87%		

2a'		σ_{Si-O}	-7.974	2			27.44%	15.38%			24.41%	15.52%
1a'		σ_{Pr-O}	-9.283	2	10.22%	1.13%	75.49%	4.38%	9.56%		76.22%	3.34%
1a''		π_{Si-O}	-9.508	2	7.86%		79.41%	7.84%	5.47%		81.96%	5.55%

Table S25. Energies and percent compositions of the occupied valence molecular orbitals of NPrO at the B3LYP and M06-HF levels of theory.

					B3LYP				M06-HF			
MOs	Isosurface	type	Energy	Occ	Pr		O	N	Pr		O	N
					5d	4f	2p	2p	5d	4f	2p	2p
2σ	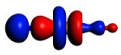	σ	-5.868	2	3.31%	58.03 %	2.51%	24.56 %	16.84 %	3.02%	35.87 %	28.52 %
2π'		π	-6.746	2	9.13%	19.53 %	7.27%	62.69 %	9.96%	11.93 %	12.33 %	63.33 %
2π		π	-6.746	2	9.13%	19.53 %	7.27%	62.69 %	9.96%	11.93 %	12.33 %	63.33 %
1σ	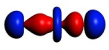	σ	-8.305	2	11.79 %	5.74%	53.28 %	16.20 %		71.60 %	19.99 %	3.47%
1π'		π	-9.112	2	15.22 %	2.38%	75.47 %	6.06%	17.26 %	1.03%	73.36 %	7.50%
1π		π	-9.112	2	15.22 %	2.38%	75.47 %	6.06%	17.26 %	1.03%	73.36 %	7.50%

Table S26. Energies and percent compositions of the occupied valence molecular orbitals of PPrO at the B3LYP and M06-HF levels of theory.

					B3LYP				M06-HF			
MOs	Isosurface	type	Energy	Occ	Pr		O	P	Pr		O	P
					5d	4f	2p	2p	5d	4f	2p	2p
2π'	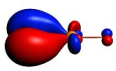	π	-5.424	2	11.71 %	10.82 %	2.38%	73.09 %	20.79 %	14.52 %	2.25%	56.15 %
2π	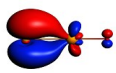	π	-5.424	2	11.71 %	10.82 %	2.38%	73.09 %	20.79 %	14.52 %	2.25%	56.15 %
2σ	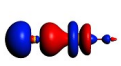	σ	-5.861	1	4.31%	45.37 %		47.21 %	4.70%	1.05%	4.28%	65.08 %
1δ	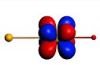	Pr-4f$_\delta$	-6.520	1		99.92 %			1.09%	91.01 %	2.06%	
1σ	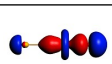	σ	-8.624	2	13.59 %	9.49%	58.74 %	9.20%	21.15 %		50.66 %	13.70 %

1π'	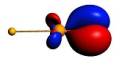	π	-9.086	2	14.10 %	4.27%	79.39 %	1.13%	15.40 %	4.93%	77.71 %	
1π	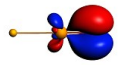	π	-9.086	2	14.10 %	4.27%	79.39 %	1.13%	15.40 %	4.93%	77.71 %	

Table S27. Energies and percent compositions of the occupied valence molecular orbitals of AsPrO at the B3LYP and M06-HF levels of theory.

					B3LYP				M06-HF			
MOs	Isosurface	type	Energy	Occ	Pr		O	As	Pr		O	As
					5d	4f	2p	2p	5d	4f	2p	2p
3a''	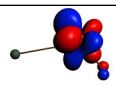	Pr-4f	-4.722	1	8.17%	87.09%	2.02%	1.46%		94.67%	3.11%	
5a'	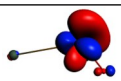	Pr-4f	-4.820	1	4.55%	83.24%		5.73%		97.18%	1.23%	
4a'	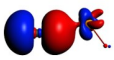	σ_{As-Pr}	-5.485	2	6.60%	5.90%		76.29%	2.56%		1.22%	81.37%
3a'		π_{As-Pr}	-5.562	1	2.60%	1.06%	3.24%	90.53%	2.36%		2.03%	92.90%
2a''		π_{As-Pr}	-5.732	1	7.71%			90.60%	5.68%			92.39%
2a'	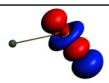	σ_{Pr-O}	-7.597	2	16.50%	5.34%	66.45%		21.64%	4.03%	64.65%	
1a'	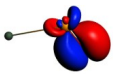	π_{Pr-O}	-8.019	2	15.36%	4.42%	76.90%	1.04%	15.93%	1.79%	78.05%	1.10%
1a''	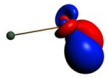	π_{Pr-O}	-8.046	2	13.58%	7.60%	76.64%		16.43%	3.14%	77.86%	

Table S28. Energies and percent compositions of the occupied valence molecular orbitals of PrO_2 at the B3LYP and M06-HF levels of theory.

					B3LYP				M06-HF			
MO s	Isosurface	typ e	Energ y	Oc c	Pr		O	O	Pr		O	O
					5d	4f	2p	2p	5d	4f	2p	2p
$1\sigma_u$	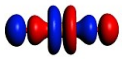	σ	-6.288	2		51.30 %	20.30 %	20.30 %	16.65 %		39.50 %	39.50 %
$1\pi_u'$	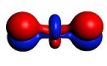	π	-7.489	2		12.22 %	42.56 %	42.56 %		9.25%	44.19 %	44.19 %
$1\pi_u$	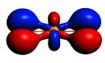	π	-7.489	2		12.22 %	42.56 %	42.56 %		9.25%	44.19 %	44.19 %
$1\sigma_g$	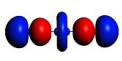	O-p_σ	-8.407	2		15.71 %	39.27 %	39.27 %		68.71 %	14.22 %	14.22 %

$1\pi_g'$	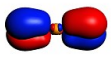	O-p_π	-8.591	2	17.97 %		40.74 %	40.74 %	16.08 %		41.94 %	41.94 %
$1\pi_g$		O-p_π	-15.681	2	17.97 %		40.74 %	40.74 %	16.08 %		41.94 %	41.94 %

Table S29. Energies and percent compositions of the occupied valence molecular orbitals of PrO_2^+ at the B3LYP and M06-HF levels of theory.

					B3LYP				M06-HF			
MOs	Isosurface	type	Energy	Occ	Pr		O	O	Pr		O	O
					5d	4f	2p	2p	5d	4f	2p	2p
$1\sigma_u$	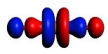	σ	-14.388	2		61.90 %	28.40 %			73.42 %	22.11 %	
$1\pi_u'$		π	-15.927	2		21.14 %	75.20 %			14.23 %	82.55 %	
$1\pi_u$	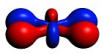	π	-15.927	2		21.14 %	75.20 %			14.23 %	82.55 %	
$1\sigma_g$	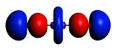	O-p_σ	-16.644	2	14.98 %			76.17 %	17.47 %			74.02 %
$1\pi_g'$		O-p_π	-17.269	2	17.88 %			81.70 %	18.73 %			80.67 %
$1\pi_g$	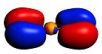	O-p_π	-17.269	2	17.88 %			81.70 %	18.73 %			80.67 %

Table S30. Energies and percent compositions of the occupied valence molecular orbitals of SPrO at the B3LYP and M06-HF levels of theory.

					B3LYP				M06-HF			
MOs	Isosurface	type	Energy	Occ	Pr		O	S	Pr		O	S
					5d	4f	2p	2p	5d	4f	2p	2p
5a'		π_{Si-Pr}	-6.019	2	5.28%	23.16%	1.36%	68.03%	5.31%	6.40%	3.23%	77.00%
2a''		π_{Si-Pr}	-6.200	2	13.13%	6.19%	1.48%	78.39%	16.84%	3.94%	1.60%	72.12%
4a'		σ_{Si-Pr}	-6.234	2	13.32%	10.86%	2.53%	67.20%	15.20%		5.85%	70.16%
3a'	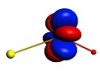	Pr-4f	-6.836	1		98.75%				66.55%		
2a'	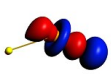	σ_{Pr-O}	-8.687	2	14.68%	7.55%	72.18%	5.44%	14.53%	2.65%	71.49%	4.45%
1a'		π_{Pr-O}	-9.083	2	8.77%	5.27%	75.82%	2.49%	16.57%	5.61%	67.64%	1.55%

1a''	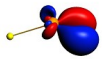	π_{Pr-O}	-9.108	2	13.77%	5.67%	77.88%		16.01%	5.46%	75.82%	

Table S31. Energies and percent compositions of the occupied valence molecular orbitals of $SPrO^+$ at the B3LYP and M06-HF levels of theory.

					B3LYP				M06-HF			
MOs	Isosurface	type	Energy	Occ	Pr		O	S	Pr		O	S
					5d	4f	2p	2p	5d	4f	2p	2p
2σ	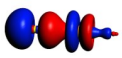	σ	-12.837	2	4.16%	49.70%		42.75%		76.52%	18.14%	
2π'	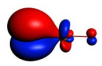	π	-12.889	2	8.09%	13.19%	1.74%	76.24%	7.05%	5.21%	4.18%	80.45%
2π		π	-12.889	2	8.09%	13.19%	1.74%	76.24%	7.05%	5.21%	4.18%	80.45%
1σ	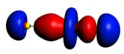	σ	-15.484	2	13.73%	10.61%	54.90%	11.66%	22.37%	6.33%	33.00%	28.45%
1π'	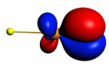	π	-16.077	2	13.34%	6.55%	77.47%	1.73%	15.11%	3.07%	78.14%	2.21%
1π	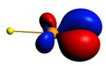	π	-16.077	2	13.34%	6.55%	77.47%	1.73%	15.11%	3.07%	78.14%	2.21%

Table S32. Energies and percent compositions of the occupied valence molecular orbitals of FPrO at the B3LYP and M06-HF levels of theory.

					B3LYP				M06-HF			
MOs	Isosurface	type	Energy	Occ	Pr		O	F	Pr		O	F
					5d	4f	2p	2p	5d	4f	2p	2p
3a''		Pr-4f	-4.282	1	13.01%	80.37%	2.35%			77.62%	2.60%	14.93%
5a'		Pr-4f	-4.585	1	2.56%	94.02%			1.93%	65.46%	5.12%	25.07%
4a'		σ_{Pr-O}	-6.997	2	10.95%	8.44%	66.91%	4.91%	19.97%	3.21%	67.19%	2.05%
3a'		π_{Pr-O}	-7.345	2	9.27%	7.74%	74.61%	4.28%	9.45%	4.40%	76.45%	4.66%
2a''		π_{Pr-O}	-7.501	2	14.40%	3.45%	78.61%		15.79%	2.49%	78.94%	
1a''		π_{F-Pr}	-9.574	2	3.35%			93.70%	2.07%			95.28%
2a'		π_{F-Pr}	-9.578	2	3.93%	1.01%	1.04%	91.30%	2.36%	12.76%		81.49%

1a'		σ_{F-Pr}	-9.790	2	6.01%	1.11%	3.31%	83.48%		34.36%	1.22%	58.54%

Table S33. Energies and percent compositions of the occupied valence molecular orbitals of F_3PrO at the B3LYP and M06-HF levels of theory.

					B3LYP				M06-HF			
MOs	Isosurface	type	Energy	Occ	Pr		O	F	Pr		O	F
					5d	4f	2p	2p	5d	4f	2p	2p
3a'		σ_{Pr-O}	-10.092	2	2.34%	14.92%	38.56%	34.04%	1.11%	28.39%	12.44%	53.28%
3a''		π_{Pr-O}	-10.497	2	1.12%	8.53%	50.57%	36.60%	1.26%	10.58%	47.74%	37.62%
2a'		π_{Pr-O}	-10.516	2		7.83%	50.59%	36.39%		10.34%	45.56%	39.63%
2a''		π_{F-Pr}	-11.628	2		8.42%	11.38%	79.58%		3.39%	12.87%	82.55%
1a'		π_{F-Pr}	-11.650	2		6.68%	12.14%	78.46%	3.67%	7.80%	9.58%	74.41%
1a''		σ_{F-Pr}	-11.693	2		6.08%		93.90%		1.37%		97.21%

Table S34. Energies and percent compositions of the occupied valence molecular orbitals of ClPrO at the B3LYP and M06-HF levels of theory.

					B3LYP				M06-HF			
MOs	Isosurface	type	Energy	Occ	Pr		O	Cl	Pr		O	Cl
					5d	4f	2p	2p	5d	4f	2p	2p
6a'	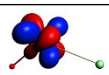	Pr-4f	-4.798	1	4.87%	93.94%				98.30%		
5a'	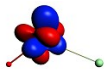	Pr-4f	-4.820	1	3.29%	92.80%			3.82%	92.73%		
4a'		σ_{Pr-O}	-7.147	2	3.70%	4.09%	39.27%	46.54%	2.48%	4.34%	36.35%	50.84%
2a''	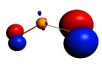	π_{Cl-Pr}	-7.590	2	3.17%		11.31%	83.34%	1.92%		5.67%	89.27%
3a'	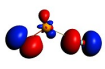	π_{Pr-O}	-7.614	2	5.93%	2.65%	48.13%	38.23%	8.12%	1.76%	36.83%	48.60%
2a'	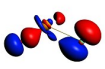	π_{Cl-Pr}	-7.902	2	10.46%		30.08%	49.51%	14.42%		47.15%	33.01%
1a''		π_{Pr-O}	-8.084	2	15.31%	4.14%	66.63%	11.77%	16.87%	1.71%	73.37%	5.64%

1a'	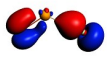	$\sigma_{Cl\text{-}Pr}$	-8.464	2	13.32%	1.23%	31.69%	50.13%	13.04%	1.32%	27.45%	51.58%

Table S35. Energies and percent compositions of the occupied valence molecular orbitals of Cl_3PrO at the B3LYP and M06-HF levels of theory.

					B3LYP				M06-HF			
MOs	Isosurface	type	Energy	Occ	Pr		O	Cl	Pr		O	Cl
					5d	4f	2p	2p	5d	4f	2p	2p
3a'		$\sigma_{Pr\text{-}O}$	-9.139	2		3.31%	6.46%	86.99%	5.12%		1.34%	82.69%
3a''		π	-9.230	2			2.13%	96.34%				96.31%
2a'		π	-9.232	2			3.05%	93.35%				95.33%
2a''		$\sigma_{Cl\text{-}Pr}$	-9.268	2		8.70%		91.20%		1.55%		96.97%
1a''		$\pi_{Cl\text{-}Pr}$	-9.575	2	2.76%	9.02%	5.76%	82.57%	5.58%		3.12%	87.65%
1a'		$\pi_{Cl\text{-}Pr}$	-9.599	2	1.91%	8.63%	4.13%	84.16%	1.04%		1.59%	92.57%

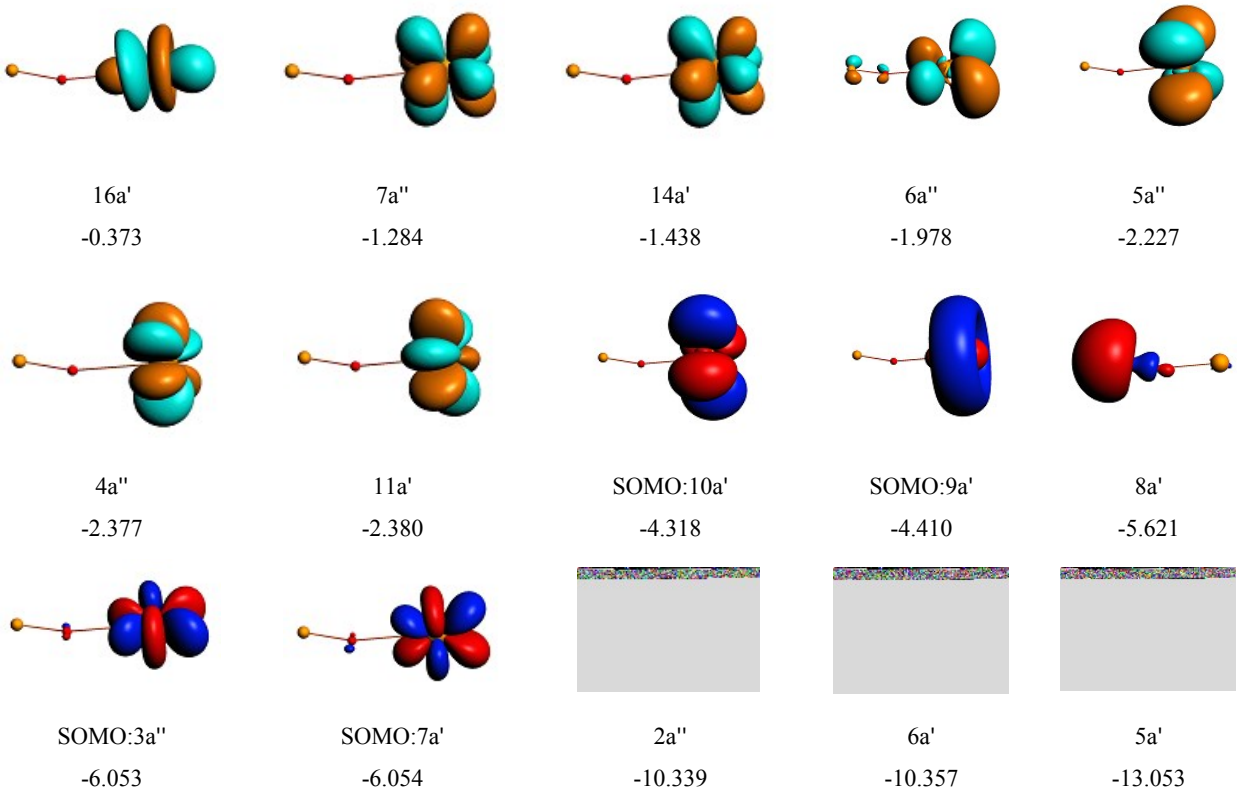

Figure S1. Frontier Kohn−Sham molecule orbitals of the BOPr complex. The value of the contour isovalues is 0.05 a.u. Only the alpha spin orbitals are presented, with the colors of blue and red for the phases of the occupied orbitals in contrast to that of yellow and cyan for the phases of the virtual orbitals.

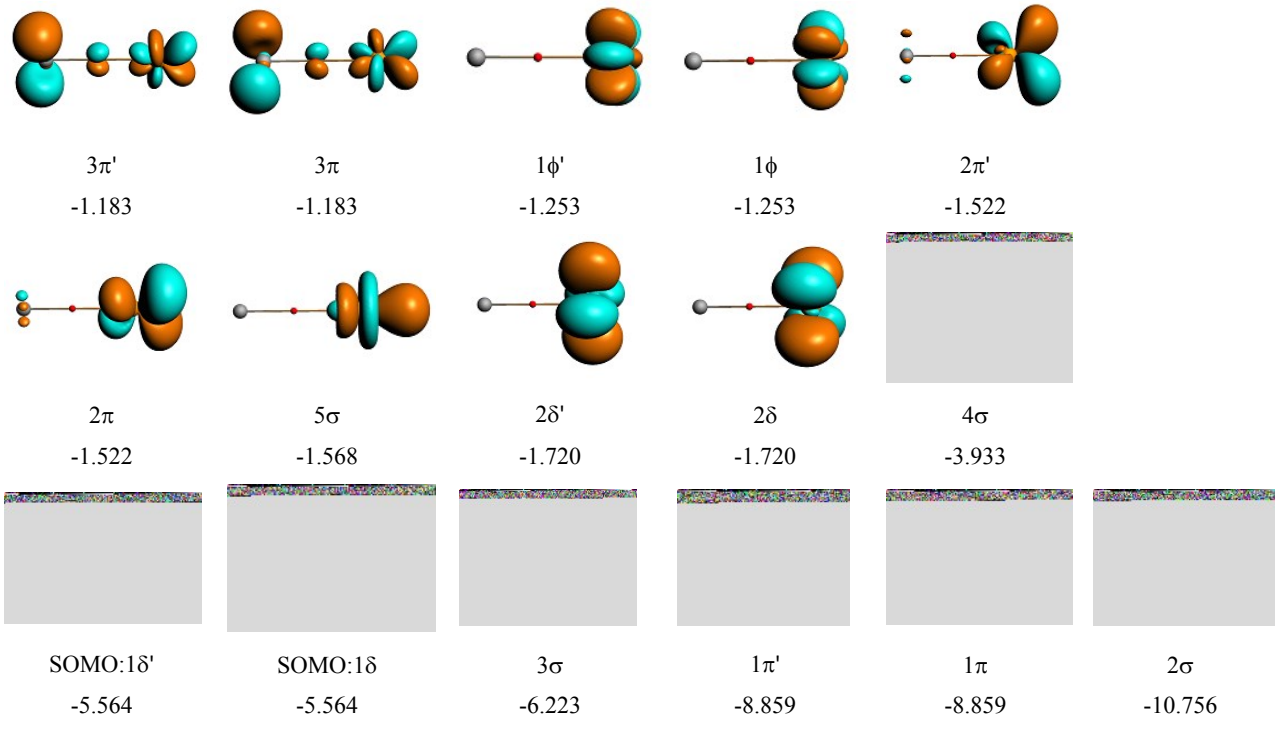

Figure S2. Frontier Kohn−Sham molecule orbitals of the AlOPr complex. The value of the contour isovalues is 0.05 a.u. Only the alpha spin orbitals are presented, with the colors of blue and red for the phases of the occupied orbitals in contrast to that of yellow and cyan for the phases of the virtual orbitals.

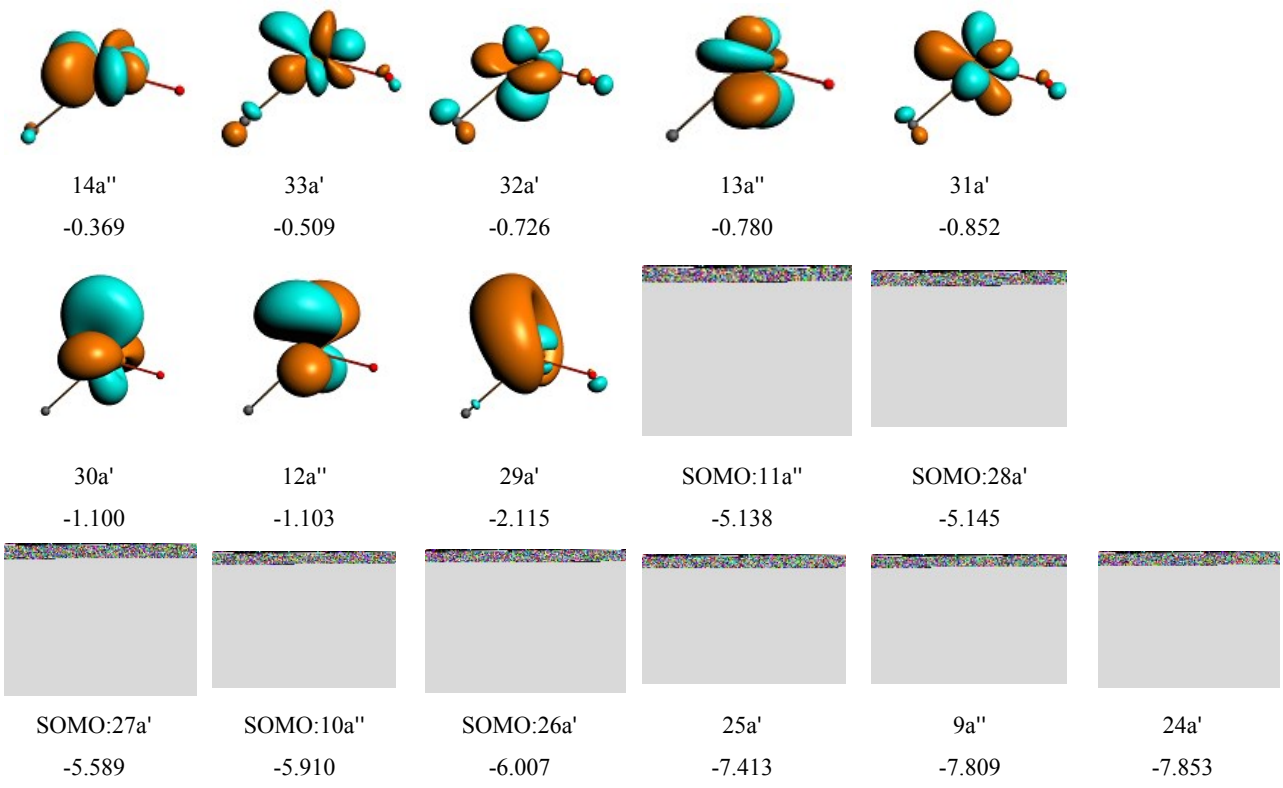

Figure S3. Frontier Kohn−Sham molecule orbitals of the CPrO complex. The value of the contour isovalues is 0.05 a.u. Only the alpha spin orbitals are presented, with the colors of blue and red for the phases of the occupied orbitals in contrast to that of yellow and cyan for the phases of the virtual orbitals.

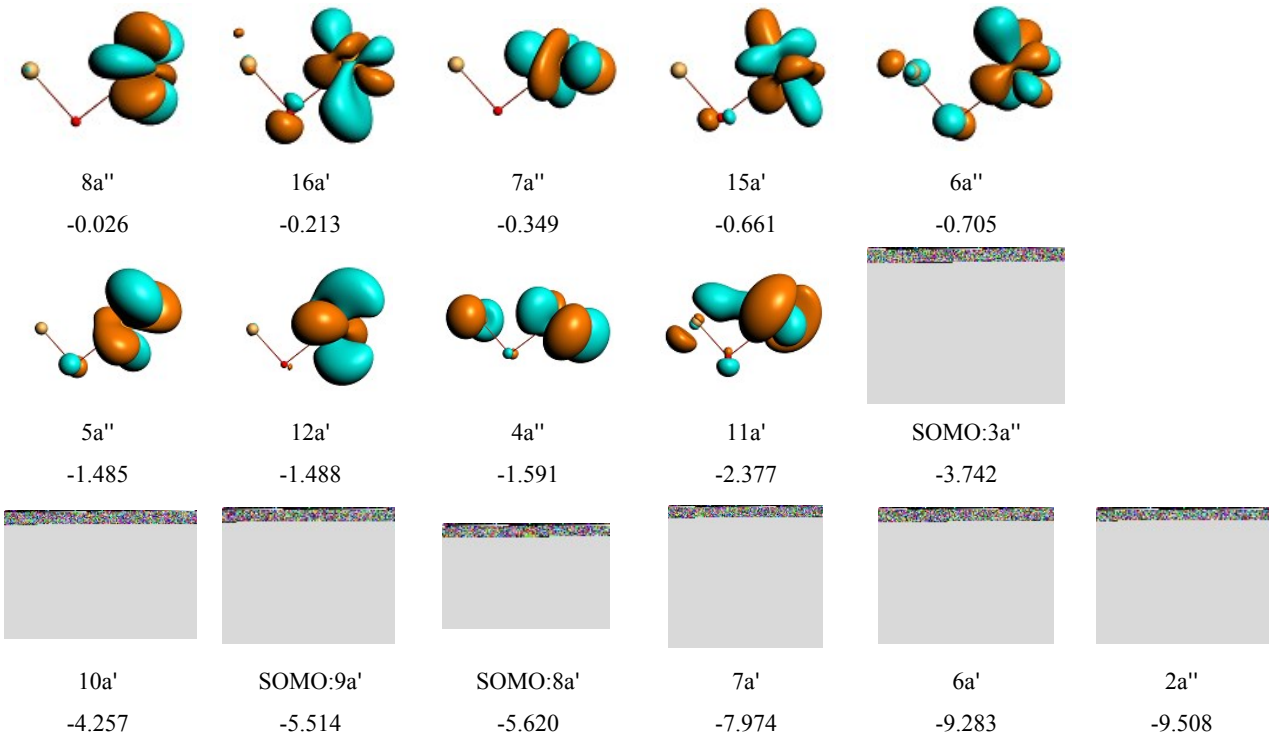

Figure S4. Frontier Kohn−Sham molecule orbitals of the SiOPr complex. The value of the contour isovalues is 0.05 a.u. Only the alpha spin orbitals are presented, with the colors of blue and red for the phases of the occupied orbitals in contrast to that of yellow and cyan for the phases of the virtual orbitals.

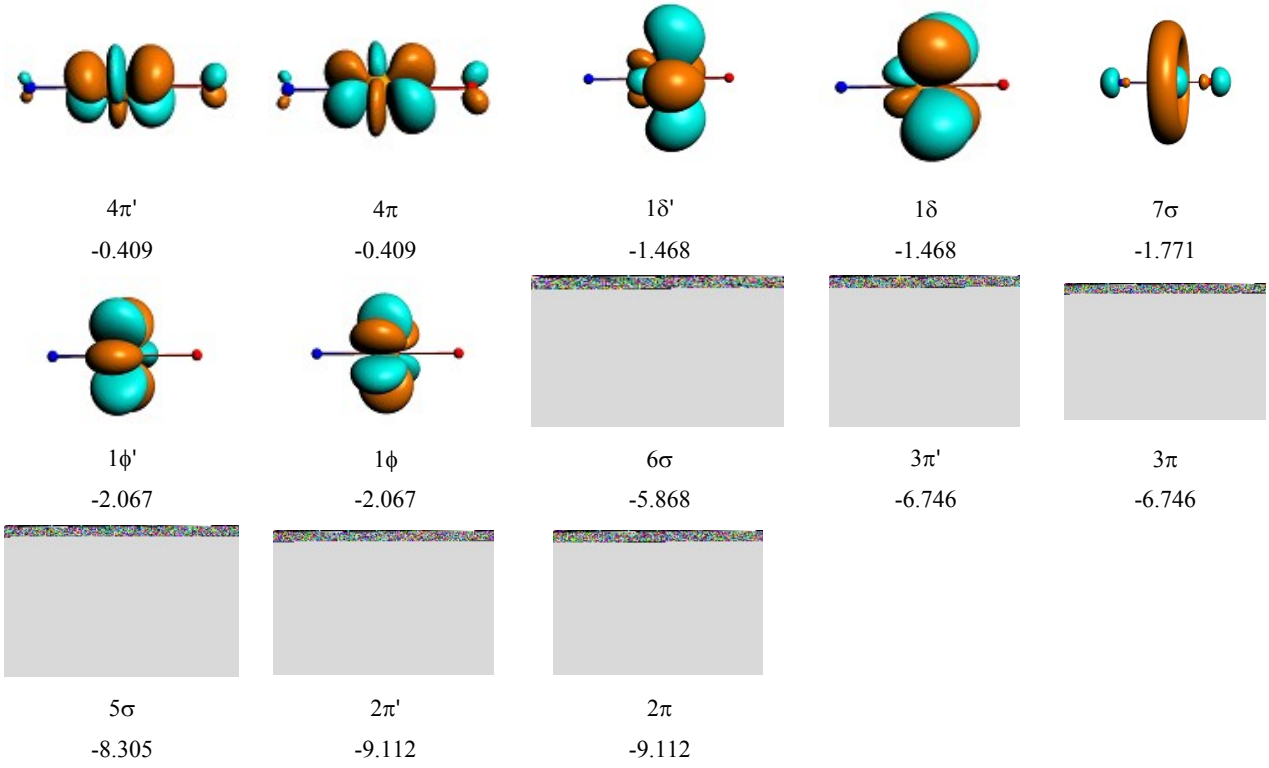

Figure S5. Frontier Kohn−Sham molecule orbitals of the NPrO complex. The value of the contour isovalues is 0.05 a.u. Only the alpha spin orbitals are presented, with the colors of blue and red for the phases of the occupied orbitals in contrast to that of yellow and cyan for the phases of the virtual orbitals.

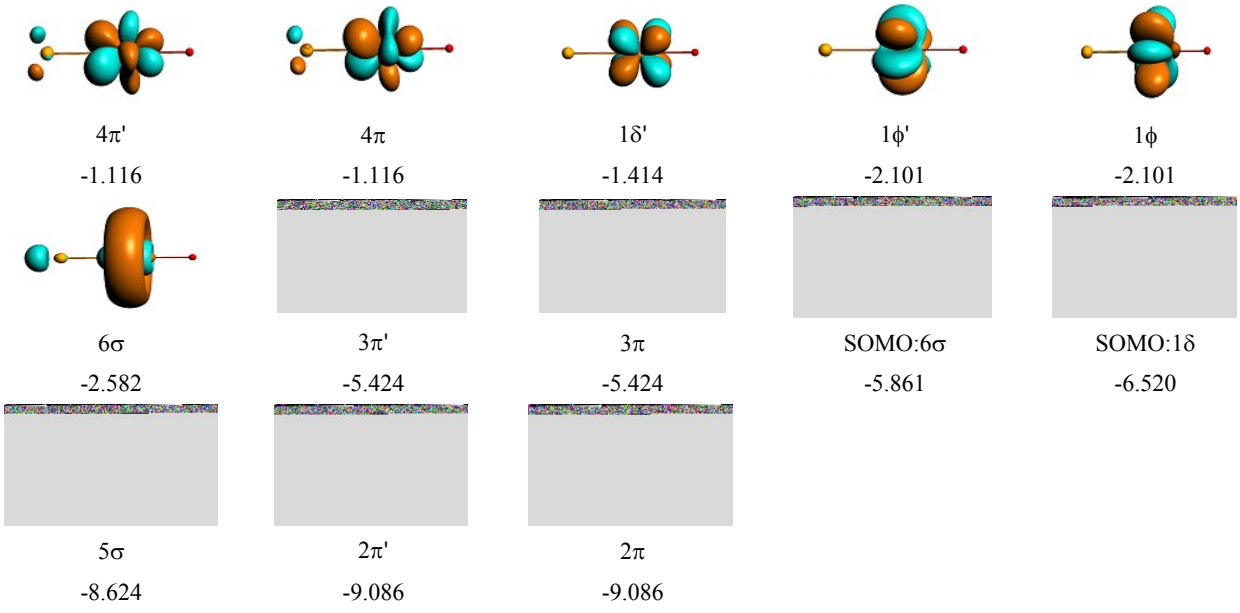

Figure S6. Frontier Kohn−Sham molecule orbitals of the PPrO complex. The value of the contour isovalues is 0.05 a.u. Only the alpha spin orbitals are presented, with the colors of blue and red for the phases of the occupied orbitals in contrast to that of yellow and cyan for the phases of the virtual orbitals.

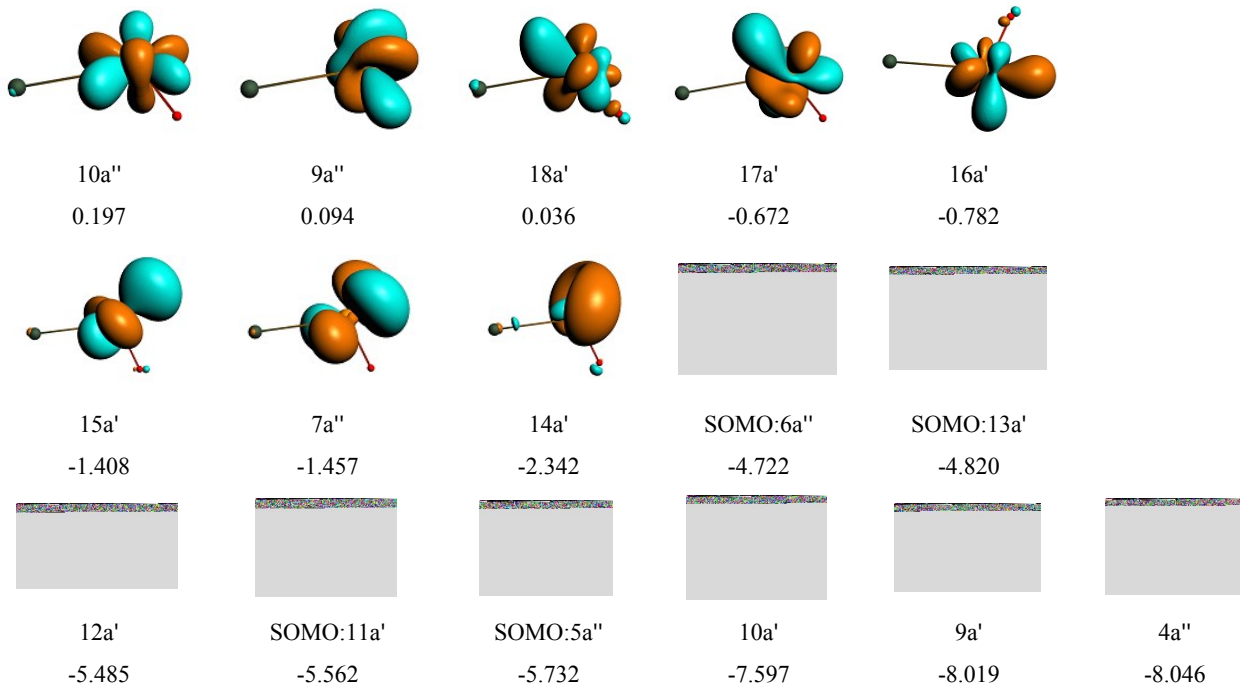

Figure S7. Frontier Kohn−Sham molecule orbitals of the AsPrO complex. The value of the contour isovalues is 0.05 a.u. Only the alpha spin orbitals are presented, with the colors of blue and red for the phases of the occupied orbitals in contrast to that of yellow and cyan for the phases of the virtual orbitals.

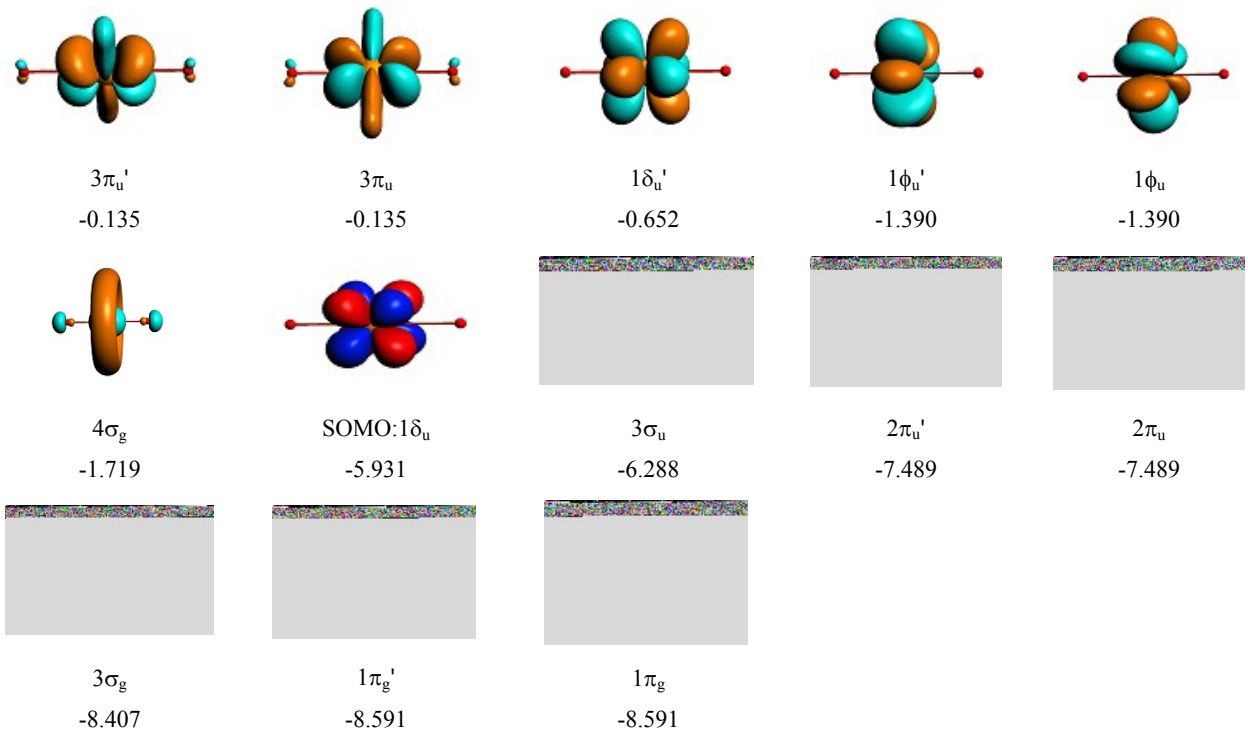

Figure S8. Frontier Kohn−Sham molecule orbitals of the PrO_2 complex. The value of the contour isovalues is 0.05 a.u. Only the alpha spin orbitals are presented, with the colors of blue and red for the phases of the occupied orbitals in contrast to that of yellow and cyan for the phases of the virtual orbitals.

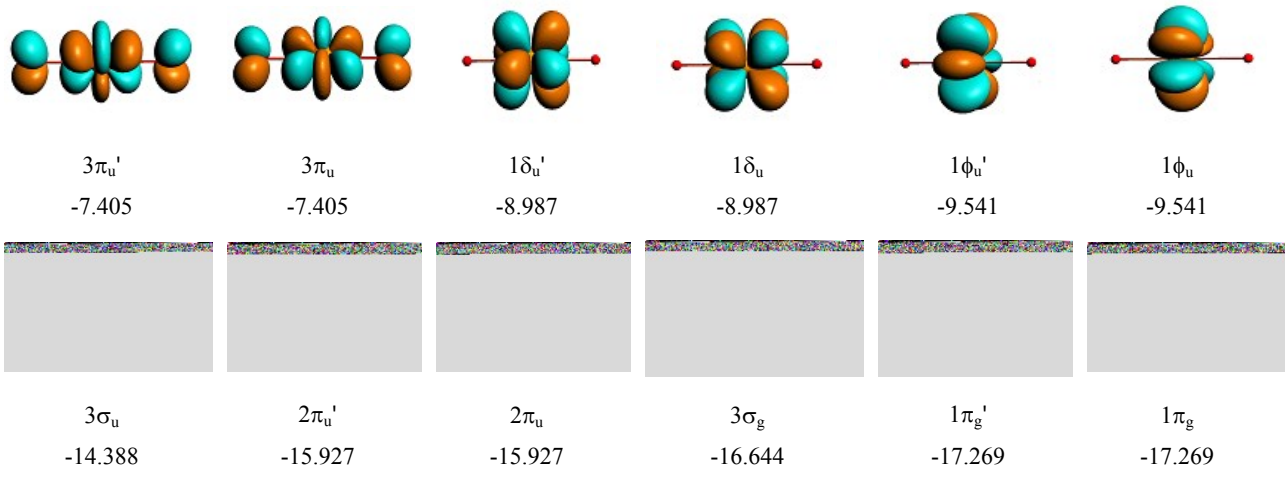

Figure S9. Frontier Kohn−Sham molecule orbitals of the $[PrO_2]^+$ complex. The value of the contour isovalues is 0.05 a.u. Only the alpha spin orbitals are presented, with the colors of blue and red for the phases of the occupied orbitals in contrast to that of yellow and cyan for the phases of the virtual orbitals.

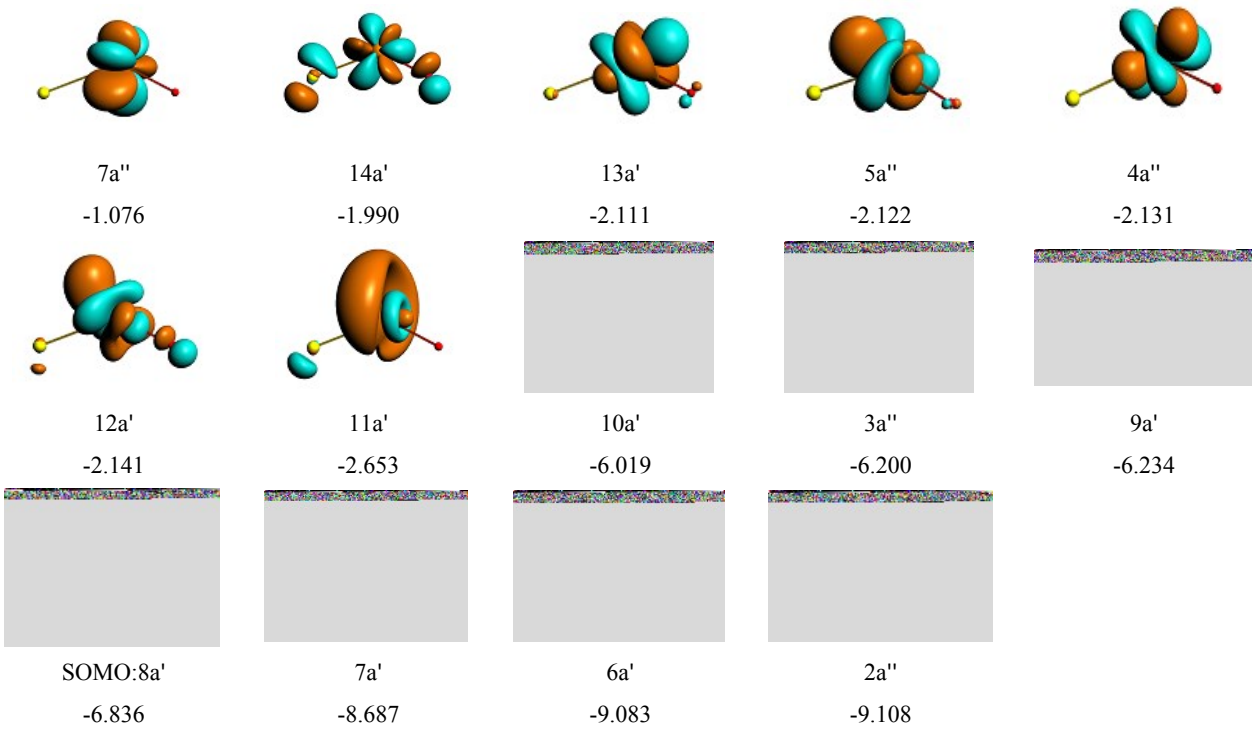

Figure S10. Frontier Kohn−Sham molecule orbitals of the SPrO complex. The value of the contour isovalues is 0.05 a.u. Only the alpha spin orbitals are presented, with the colors of blue and red for the phases of the occupied orbitals in contrast to that of yellow and cyan for the phases of the virtual orbitals.

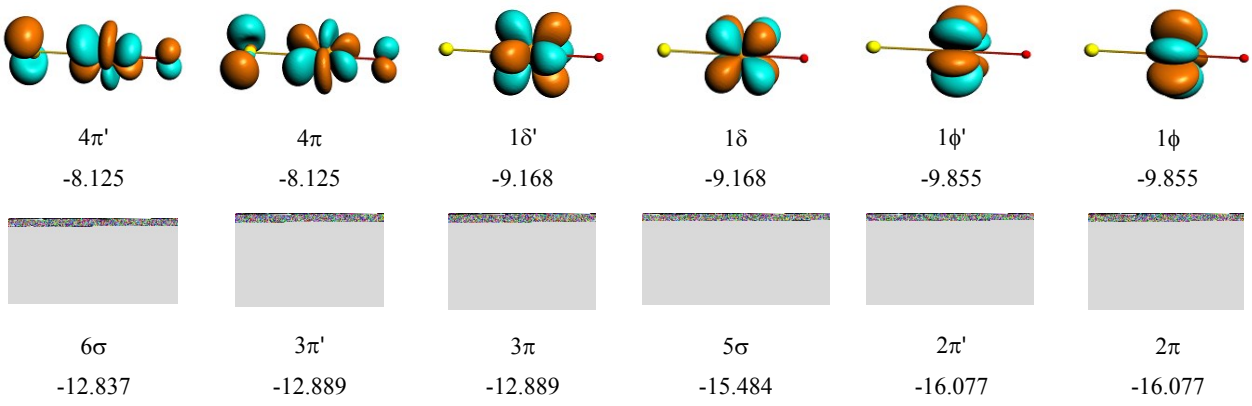

Figure S11. Frontier Kohn−Sham molecule orbitals of the $[SPrO]^+$ complex. The value of the contour isovalues is 0.05 a.u. Only the alpha spin orbitals are presented, with the colors of blue and red for the phases of the occupied orbitals in contrast to that of yellow and cyan for the phases of the virtual orbitals.

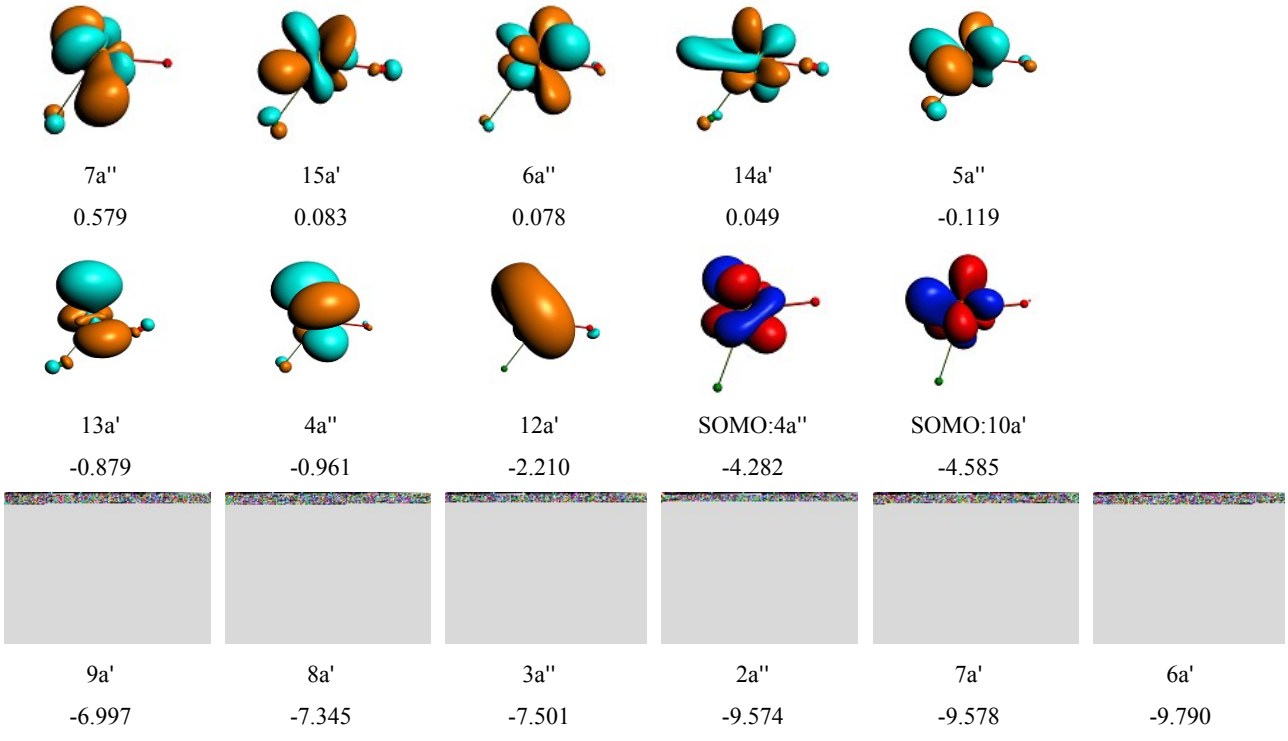

Figure S12. Frontier Kohn−Sham molecule orbitals of the FPrO complex. The value of the contour isovalues is 0.05 a.u. Only the alpha spin orbitals are presented, with the colors of blue and red for the phases of the occupied orbitals in contrast to that of yellow and cyan for the phases of the virtual orbitals.

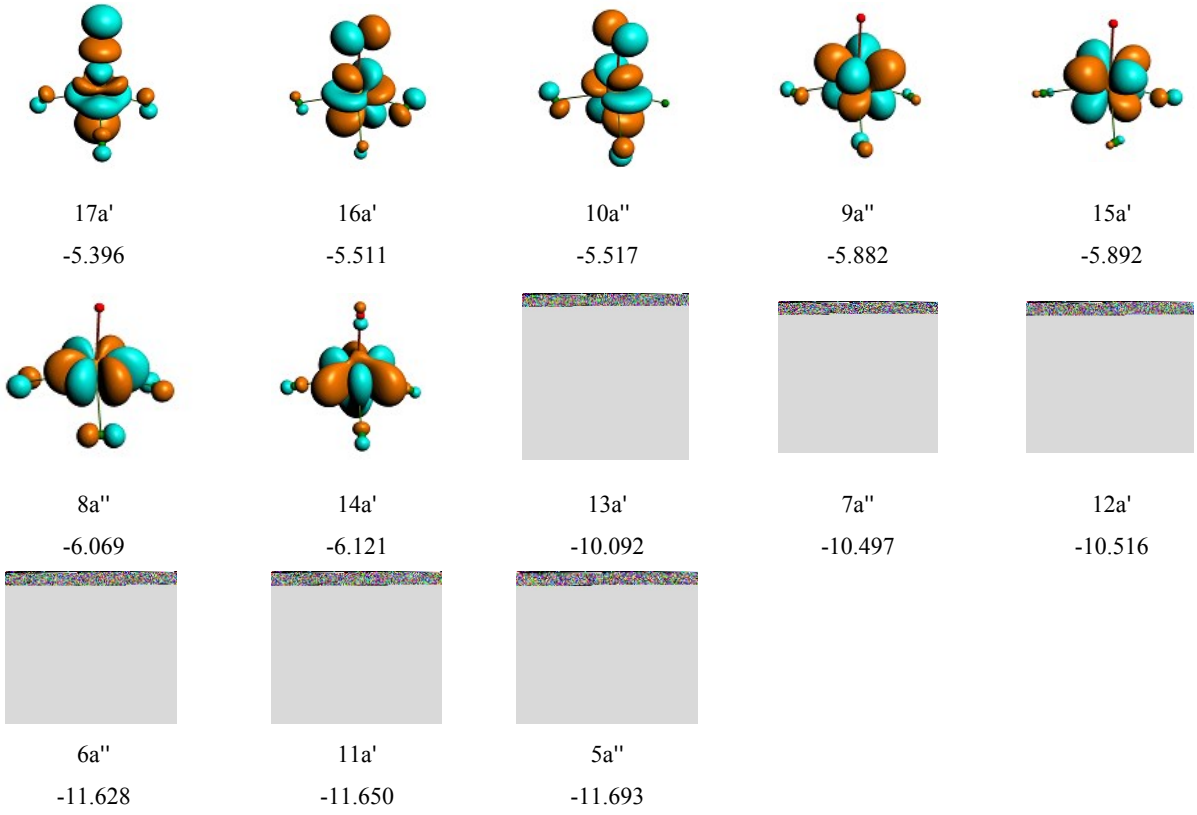

Figure S13. Frontier Kohn−Sham molecule orbitals of the F_3PrO complex. The value of the contour isovalues is 0.05 a.u. Only the alpha spin orbitals are presented, with the colors of blue and red for the phases of the occupied orbitals in contrast to that of yellow and cyan for the phases of the virtual orbitals.

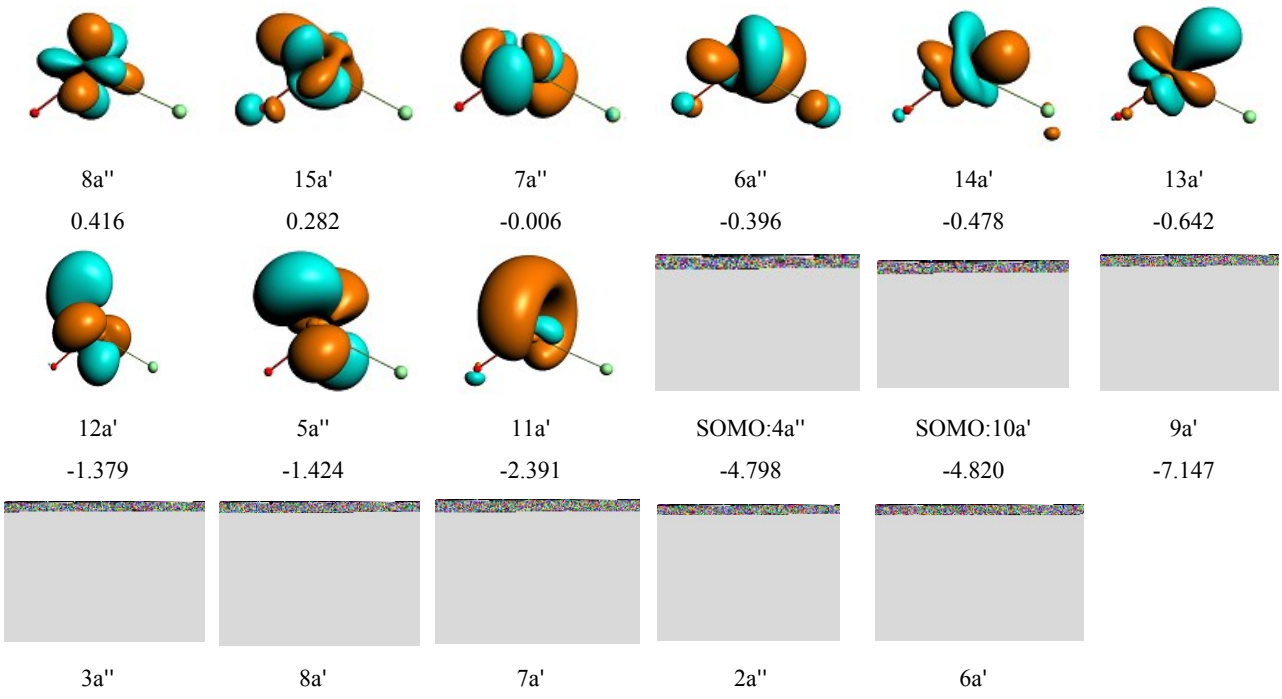

-7.590 -7.614 -7.902 -8.084 -8.464

Figure S14. Frontier Kohn−Sham molecule orbitals of the ClPrO complex. The value of the contour isovalues is 0.05 a.u. Only the alpha spin orbitals are presented, with the colors of blue and red for the phases of the occupied orbitals in contrast to that of yellow and cyan for the phases of the virtual orbitals.

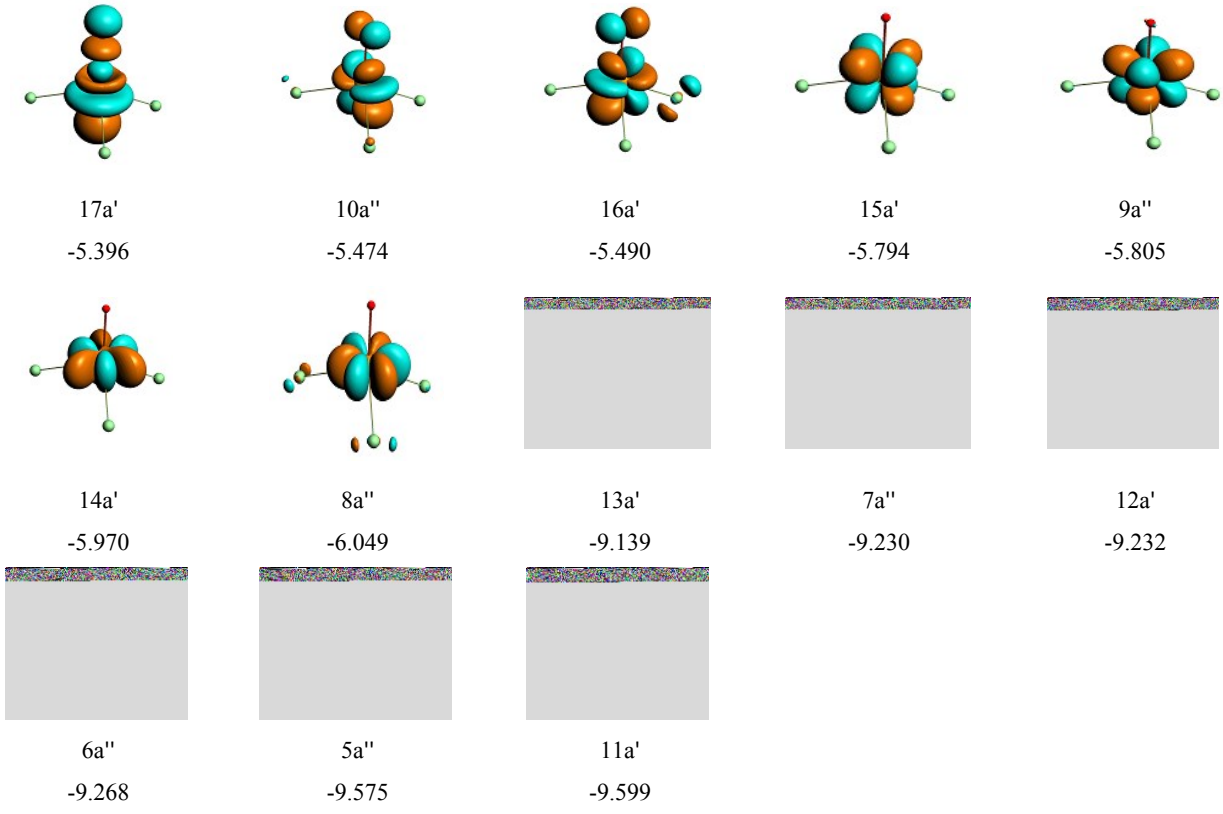

Figure S15. Frontier Kohn−Sham molecule orbitals of the Cl_3PrO complex. The value of the contour isovalues is 0.05 a.u. Only the alpha spin orbitals are presented, with the colors of blue and red for the phases of the occupied orbitals in contrast to that of yellow and cyan for the phases of the virtual orbitals.

Reference

1. S.-X. Hu, J. Jian, J. Su, X. Wu, J. Li and M. Zhou, Chem. Sci., 2017,8, 4035–4043.
2. Q. Zhang, S. X. Hu, H. Qu, J. Su, G. Wang, J. B. Lu, M. Chen, M. Zhou and J. Li, *Angew. Chem.-Int. Edit.*, 2016, **55**, 6896–6900.
3. T. Mikulas, M. Y. Chen, D. A. Dixon, K. A. Peterson, Y. Gong and L. Andrews, *Inorg. Chem.*, 2014, **53**, 446–456.